www.oeaw.ac.at

Johann Radon Institute for
Computational and Applied Mathematics
Austrian Academy of Sciences (ÖAW)

Shape optimization approaches to Free Surface Problems

H. Kasumba

RICAM-Report 2013-17

SHAPE OPTIMIZATION APPROACHES TO FREE SURFACE PROBLEMS

H. KASUMBA

Abstract. Three different reformulations of a free surface problem as shape optimization problems are considered. These give rise to three different cost functionals which apparently have not been exploited in literature. The shape derivatives of the cost functionals are explicitly determined. The gradient information is combined with the boundary variation method in a steepest descent algorithm to solve the shape optimization problems. Numerical results which compare the performance of the proposed cost functionals are presented.

1. Introduction

The numerical solution of flows which are partially bounded by a freely moving boundary is of great practical importance, e.g., in coating flows [25], thin film manufacturing processes [38], ship hydrodynamics [1], and continuous casting of steel [31]. Such problems have an inherent difficulty in that the flow domain as well as the flow variables need to be determined simultaneously, which implies that a numerical solution has to be carried out iteratively [18]. In recent years several techniques were developed for the solution of free surface flow problems. These techniques are roughly classified by [39, et al] as Eulerian, Lagrangian or mixed Eulerian-Lagrangian.

In Eulerian-like (volume-tracking) approaches, the mesh remains stationary and the free surface is not explicitly tracked. Rather, it is reconstructed from other field properties such as the fluid fractions, which can be determined as the fluid moves in/out of the computational flow domain. Methods that fall into this category include the finite-difference-based marker-and-cell methods [28], level-set methods [30, 27], and volume-of-fluid methods [5, 15].

In Lagrangian-like approaches, the grid points move with the local fluid particles, so the free surface is sharply defined. However, mesh refinement or remeshing is usually necessary for large deformations, e.g., see [22]. Solution strategies that fall into the second category described above are of particular interest in this work. These strategies include fixed point methods [20, 32, 37], total linearization methods (continuous or discrete)[7], and shape optimization methods [36, 19, 35].

The fixed point method assigns a shape to the free boundary and the PDE is solved for this shape after either the kinematic or the dynamic boundary condition on the free boundary is disregarded. Next, a new shape of the free boundary is computed such that the error in the extra boundary condition is minimized. This procedure is repeated until convergence is attained. The approach does not require gradient information, however, as pointed out in [35], the convergence of this type of scheme depends sensitively on parameters in the problem.

Key words and phrases. Free surface flow, Shape optimization, Shape derivative.

A method that counters the deficiencies of the aforementioned approach is the total linearization method. This method is a form of Newton-type iteration on a full set of equations, i.e., the location of the free boundary and as well as the flow variables. Since all unknowns are treated at once in a single iteration, this method is infeasible for problems with many unknowns [36, 35].

Next, we turn to the shape optimization approach that we follow in this work. Since free surface problems have an over determined number of boundary conditions on the free-boundary, they can be reformulated into an equivalent shape optimization problem. The problem now consists in finding the boundary that minimizes a norm of the residual of one of the free-surface conditions, subject to the boundary value problem with the remaining free-surface conditions imposed. In most of the previous work, for instance, [36, 19, 35], it is assumed that the flow is inviscid and irrotational. Consequently, this reduces the Navier-Stokes equations to free-surface potential flow equations which is much simpler to handle. This assumption is not considered in this work but rather we consider a steady free surface problem governed by the Stokes equations. We reformulate this problem into equivalent shape optimization problems by introducing three different cost functionals, namely, a least-squares energy variational functional (which is the analogue of the Kohn-Vogelius functional for the Laplacian [23]), a Dirichlet data tracking functional, and a Neumann data tracking functional.

We now turn to the discussion of the choice of cost functionals. We begin with the least-squares energy cost functional. This functional was first proposed by Kohn and Vogelius [23] in the context of the inverse conductivity problem. Recently, the authors in [4] reconstructed the shape of an obstacle immersed in a Stokes flow by utilizing the tools of shape optimization and minimizing the Kohn-Vogelius type least-squares energy functional. In [11] and recently in [3], the authors utilized this cost functional for the numerical solution of the Bernoulli free boundary problem on star-like and general shapes, respectively. In the present work, we utilize the functional to solve vector-valued free surface problems defined not only on star-like shapes but also on general shapes. We believe that reformulating free-surface problem in terms of PDE-constrained shape optimization problem where the cost is the least-squares energy cost functional penalizing the L^2-distance of the gradients of pure Dirichlet and Neumann data is novel in our work. The present reformulation seems to be advantageous in the sense that it leads to the tracking boundary data in their natural norms [11].

As an alternative to the above cost, one can utilize an L^2-Dirichlet and Neumann data tracking functional. Although it seems natural to utilize such cost functionals, we are not aware of a paper that employs shape calculus on these functionals to solve the free surface problem under consideration. A comparison among the three cost functionals is made using two test problems.

For the numerical solution of the resultant shape optimization problems, we apply a steepest descent type method, which requires the shape gradient of the cost functionals. The technique we employ to compute these gradients requires the use of the implicit function theorem and some of the ideas suggested in [16].

The continuous formulations are discretized and numerical algorithms for solving the discrete shape optimization problems are developed and implemented.

The remainder of the paper is organized as follows: In Section 2 the equations governing the steady free-surface flow and the associated shape optimization problem are stated. Section 3 describes the weak formulation and solvability of the state equations. Section 4 examines the sensitivity of the cost functionals with respect to the domain. Numerical experiments and results are presented in Section 5. Section 6 contains concluding remarks.

2. Problem set up

2.1. **Notations.** Here we collect some notations and definitions that we need in our subsequent work. Throughout the paper we restrict ourselves to the two dimensional case. We use bold fonts for vectors and vector-valued functions are also indicated by bold letters. Two notations for the inner product in $\mathbb{R}^2$ shall be used, namely (x,y) and $x \cdot y$, respectively, the latter in case of nested inner products. The unit outward normal and tangential vectors to a domain Ω shall be denoted by $\mathbf{n} = (n_1, n_2)$ and $\boldsymbol{\tau} = (-n_2, n_1)$, respectively. For a given matrix A, we denote by A^t its transpose and by A^{-t} the transpose of its inverse. For a vector valued function $\mathbf{u}$, the gradient of $\mathbf{u}$, denoted by $\nabla\mathbf{u}$, is a second order tensor defined as $\nabla\mathbf{u} = [\nabla\mathbf{u}]_{ij} := \left(\frac{\partial u_j}{\partial x_i}\right)_{i,j=1,2}$, where $[\nabla\mathbf{u}]_{ij}$ is the entry at the intersection of the i^{th} row and j^{th} column, while the Jacobian of $\mathbf{u}$, denoted by $D\mathbf{u}$, is the transpose of the gradient. Furthermore, we define the tensor scalar product denoted by $\nabla\mathbf{u} : \nabla\boldsymbol{\psi}$ as

$$\nabla\mathbf{u} : \nabla\boldsymbol{\psi} := \left(\sum_{i,j=1}^{d} \frac{\partial u_j}{\partial x_i} \frac{\partial v_j}{\partial x_i} \right) \in \mathbb{R}.$$

We denote by $H^m(\mathcal{S})$, $m \in \mathbb{R}$, the standard Sobolev space of order m defined by

$$H^m(\mathcal{S}) := \left\{ u \in L^2(\mathcal{S}) \mid D^\alpha u \in L^2(\mathcal{S}), \text{ for } 0 \le |\alpha| \le m \right\},$$

where D^α is the weak (or distributional) partial derivative, and α is a multi-index. Here $\mathcal{S}$, which is either the flow domain Ω, or its boundary Γ, or part of its boundary. The norm $\|\cdot\|_{H^m(\mathcal{S})}$ associated with $H^m(\mathcal{S})$ is given by

$$\|u\|^2_{H^m(\mathcal{S})} = \sum_{|\alpha| \le m} \int_{\mathcal{S}} |D^\alpha u|^2 \, dx.$$

Note that $H^0(\mathcal{S}) = L^2(\mathcal{S})$ and $\|\cdot\|_{H^0(\mathcal{S})} = \|\cdot\|_{L^2(\mathcal{S})}$. For vector valued functions, we define the Sobolev space $\mathbf{H}^m(\mathcal{S})$ by

$$\mathbf{H}^m(\mathcal{S}) := \{ \mathbf{u} = (u_1, u_2) \mid u_i \in H^m(\mathcal{S}), \text{ for } i = 1, 2 \},$$

and its associated norm

$$\|\mathbf{u}\|^2_{\mathbf{H}^m(\mathcal{S})} = \sum_{i=1}^{2} \|u_i\|^2_{H^m(\mathcal{S})}.$$

The tangential gradient $\nabla_\Gamma \mathbf{v}$ of a vector $\mathbf{v} \in \mathcal{C}^1(\mathbb{R}^2, \mathbb{R}^2)$ is defined as

$$\nabla_\Gamma \mathbf{v} := D\mathbf{v}|_\Gamma - (D\mathbf{v} \cdot \mathbf{n})\mathbf{n}, \tag{1}$$

and the tangential divergence $\mathrm{div}_\Gamma(\mathbf{v})$ is defined as

$$\mathrm{div}_\Gamma(\mathbf{v}) := \mathrm{div}(\mathbf{v}) - D\mathbf{v}\,\mathbf{n} \cdot \mathbf{n}. \tag{2}$$

2.2. **State problem.** Let Ω be a connected bounded domain in $\mathbb{R}^2$ with a sufficiently regular (Figure 1 (a)) or piecewise regular (Figure 1 (b)) boundary $\partial\Omega = \Gamma$.

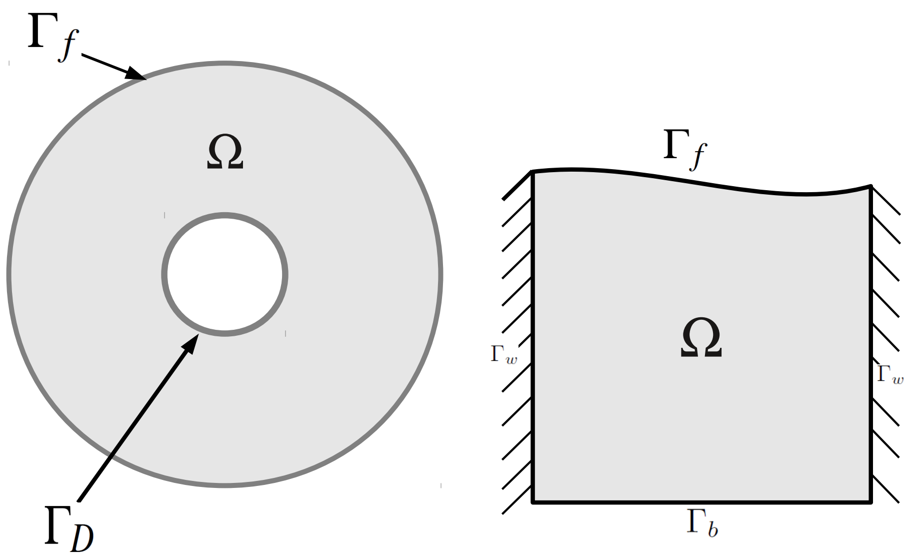

(a) Problem 1 (b) Problem 2

Figure 1. Domains for test problems

Suppose that an incompressible viscous flow occupies Ω, and that the state equation for the flow is given by the following system of Stokes equations in non-dimensional form:

$$\begin{cases} -\alpha\Delta\mathbf{u} + \nabla p = \mathbf{f} \text{ in } \Omega, \\ \operatorname{div} \mathbf{u} = 0 \text{ in } \Omega. \end{cases} \tag{3}$$

Here $\mathbf{u} = (u_1, u_2)$ is the velocity field, p the pressure, $\alpha := \frac{1}{Re} > 0$, where Re is the Reynolds number of the flow, and $\mathbf{f}$ the density of external forces.

In order to make (3) well-posed, we have to impose appropriate boundary conditions. In this work, different boundary conditions posed on the domains shown in Figure (1(a)-(b)) are considered, giving rise to 2 different test problems.

In the first test case (Fig.1 (a)), a gravity like force $\mathbf{f}$, keeps the fluid on top of the circular domain and the motion of the fluid is triggered by an initial velocity [6]. We impose the inhomogenous Dirichlet boundary conditions on the fixed boundary Γ_D:

$$\mathbf{u} = \mathbf{g} \quad \text{on} \quad \Gamma_D, \tag{4}$$

while on Γ_f, which is the free surface in this case, we assume zero ambient pressure and negligible surface tension effects. Consequently, the boundary conditions corresponding to the kinematic, normal and tangential stress balances can be expressed as

$$\begin{cases} -p\mathbf{n} + \alpha \frac{\partial \mathbf{u}}{\partial \mathbf{n}} = 0 \quad \text{on} \quad \Gamma_f, \\ \mathbf{u}\cdot\mathbf{n} = 0, \quad \text{on} \quad \Gamma_f. \end{cases} \tag{5}$$

We next turn to the second test example. For this case, we consider a two dimensional cavity with fixed vertical side walls, a driven floor, and a free surface at the upper boundary, the geometry being shown in Figure 1 (b). On $\Gamma_D := \Gamma_w \cup \Gamma_b$, we impose the following boundary conditions:

$$\begin{aligned} &\mathbf{u} = \mathbf{g}, \quad \text{on} \ \Gamma_b, \\ &\mathbf{u}\cdot\mathbf{n} = 0, \quad \alpha\frac{\partial \mathbf{u}}{\partial \mathbf{n}}\cdot\boldsymbol{\tau} = 0, \quad \text{on} \quad \Gamma_w, \end{aligned} \tag{6}$$

and on Γ_f, boundary conditions analogous to the ones in (5) are imposed. Note that a slip boundary condition is imposed on Γ_b to avoid a stress singularity that would result at contact points where the boundaries Γ_b and Γ_f, meet.

2.3. **Optimization problem.** The over-specification of boundary conditions on Γ_f naturally suggests to formulate the two test problems ((3), (4), (5)) and ((3), (5), (6)) as optimization problems; this approach has been used for potential free surface flows in e.g., [36, 35]. Here and in what follows, we shall consider for the sake of simplicity of presentation, the first test problem. The free boundary problem now consists in finding a domain Ω and an associated flow field $(\mathbf{u}, p)$ such that the following overdetermined problem is satisfied

$$\begin{cases} -\alpha\Delta\mathbf{u} + \nabla p = \mathbf{f} \quad \text{in} \quad \Omega, \\ \operatorname{div}\mathbf{u} = 0 \quad \text{in} \quad \Omega, \\ \mathbf{u} = \mathbf{g} \quad \text{on} \quad \Gamma_D, \\ -p\mathbf{n} + \alpha\frac{\partial \mathbf{u}}{\partial \mathbf{n}} = 0 \quad \text{on} \quad \Gamma_f, \\ \mathbf{u}\cdot\mathbf{n} = 0, \quad \text{on} \quad \Gamma_f. \end{cases} \tag{7}$$

There are several ways to transform the free surface problem (7) into a shape optimization problem. In this work, we will consider the following three formulations, where the infimum has always to be taken over all sufficiently smooth domains.

(i) A variational least-squares cost functional,

$$J_1(\Omega) := \frac{\alpha}{2}\int_\Omega |\nabla(\mathbf{u}_D - \mathbf{u}_N)|^2 \, d\Omega \to \inf, \tag{8}$$

where the auxiliary functions $\mathbf{u}_D$ and $\mathbf{u}_N$, satisfy

$$\begin{cases} -\alpha\Delta\mathbf{u}_D + \nabla p_D = \mathbf{f} \quad \text{in} \quad \Omega, \\ \operatorname{div}\mathbf{u}_D = 0 \quad \text{in} \quad \Omega, \\ \mathbf{u}_D = \mathbf{g} \quad \text{on} \quad \Gamma_D, \\ \mathbf{u}_D\cdot\mathbf{n} = 0, \quad \text{on} \quad \Gamma_f, \\ \alpha\frac{\partial \mathbf{u}_D}{\partial \mathbf{n}}\cdot\boldsymbol{\tau} = 0, \quad \text{on} \quad \Gamma_f, \end{cases} \tag{9}$$

and

$$
\begin{cases} -\alpha \Delta \mathbf{u}_N + \nabla p_N = \mathbf{f} \quad \text{in} \quad \Omega, \\ \operatorname{div} \mathbf{u}_N = 0 \quad \text{in} \quad \Omega, \\ \mathbf{u}_N = \mathbf{g} \quad \text{on} \quad \Gamma_D, \\ -p_N \mathbf{n} + \alpha \frac{\partial \mathbf{u}_N}{\partial \mathbf{n}} = 0 \quad \text{on} \quad \Gamma_f, \end{cases} \tag{10}
$$

is considered as the first formulation.

(ii) One can also consider the solution $\mathbf{u}_N$ of the Neumann problem (10) and track the Dirichlet data in a least-squares sense relative to $L^2(\Gamma_f)$, that is

$$
J_2(\Omega) = \frac{1}{2} \int_{\Gamma_f} (\mathbf{u}_N \cdot \mathbf{n})^2 \, d\Gamma \to \inf. \tag{11}
$$

(iii) Correspondingly, if the pure Dirichlet data is assumed to be prescribed, then we can track the Neumann boundary condition at Γ_f in the $L^2(\Gamma_f)$ least square sense, i.e.,

$$
J_3(\Omega) = \frac{1}{2} \int_{\Gamma_f} (-p_D \mathbf{n} + \alpha \frac{\partial \mathbf{u}_D}{\partial \mathbf{n}})^2 \, d\Gamma \to \inf. \tag{12}
$$

Note that this cost functional requires more regularity for p_D and $\mathbf{u}_D$ to be well-defined. Therefore, it may be impractical to use this functional in numerical experiments where high regularity of the state variables is not guaranteed. We shall turn to this issue in Section 5.

Remark 2.1. *Other types of penalization may be considered. For instance one may choose to penalize instead of J_1, by the cost functional*

$$
J_4(\Omega) := \frac{\alpha}{2} \int_{\Omega} (\boldsymbol{u}_D - \boldsymbol{u}_N)^2 \, d\Omega. \tag{13}
$$

Compared to J_1, its shape gradient would be numerically expensive to evaluate. In the case of the Bernoulli free boundary problem, it is found in [24] *that one needs to solve 5 PDES, namely, i) two state equations, ii) two adjoint equations and iii) evaluate the mean curvature κ of the free boundary, which is infeasible in the case where (9) and* (10) *are the PDE constraints.*

3. Weak formulation and solvability of the state equations

In this section we analyze the solvability of the state equations (9) and (10). For both PDEs, the analysis is presented based on homogenous Dirichlet boundary conditions on Γ_D. Extension to non-homogeneous Dirichlet boundary conditions can be accomplished by standard techniques. In order to present the weak formulation of problems (9) and (10), we introduce the functional spaces:

$$
\begin{aligned}
L^2_0(\Omega) : &= \{w \in L^2(\Omega) \ : \ \int_\Omega w \, dx = 0\},\\
W(\Omega) : &= \{\mathbf{u} \in \mathbf{H}^1(\Omega) : \ \mathbf{u}\cdot\mathbf{n} = 0 \text{ on } \Gamma_f, \ \mathbf{u} = 0 \text{ on } \Gamma_D\},\\
W_r(\Omega) : &= \{\mathbf{u} \in \mathbf{H}^1(\Omega) : \ \mathbf{u}\cdot\mathbf{n} = r \text{ on } \Gamma_f, \ \mathbf{u} = 0 \text{ on } \Gamma_D\},\\
Z(\Omega) : &= \{\mathbf{u} \in \mathbf{H}^1(\Omega) \ : \ \ \mathbf{u} = 0 \text{ on } \Gamma_D\}.
\end{aligned}
$$

We assume that the data $\mathbf{f} \in \mathbf{L}^2(\Omega)$ and that the domain Ω is of class $C^{1,1}$.

The weak formulation of (9) can be expressed as:

Find $\bar{\mathbf{x}}:=(\mathbf{u}_D, p_D) \in X := W(\Omega)\times L^2_0(\Omega)$ such that

$$
\langle E_1(\bar{\mathbf{x}},\Omega),\Theta\rangle_{X^*\times X} := \alpha(\nabla\mathbf{u}_D,\nabla\boldsymbol{\psi})_\Omega - (p_D, \text{div }\boldsymbol{\psi})_\Omega - (\text{div }\mathbf{u}_D, \xi)_\Omega - (\mathbf{f},\boldsymbol{\psi})_\Omega = 0, \tag{14}
$$

for all $\Theta := (\boldsymbol{\psi},\xi) \in X$. Analogously, the weak form of (10) can be expressed as:

Find $\bar{\mathbf{y}} := (\mathbf{u}_N, p_N) \in Y := Z(\Omega)\times L^2(\Omega)$ such that

$$
\langle E_2(\bar{y},\Omega),\Psi\rangle_{Y^*\times Y} := \alpha(\nabla\mathbf{u}_N,\nabla\boldsymbol{\varphi})_\Omega - (p_N, \text{div }\boldsymbol{\varphi})_\Omega - (\text{div }\mathbf{u}_N, \zeta)_\Omega - (\mathbf{f},\boldsymbol{\varphi})_\Omega = 0, \tag{15}
$$

for all $\Psi := (\boldsymbol{\varphi},\zeta) \in Y$.

It is known (see, e.g., [26]) that (14) possesses a unique solution $\bar{\mathbf{x}}:=(\mathbf{u}_D, p_D) \in X$. Furthermore, following [4], it can be shown that (15) possesses a unique solution $\bar{\mathbf{y}}:=(\mathbf{u}_N, p_N) \in Y$. Moreover since Ω is of class $C^{1,1}$, we have that

$$
\bar{\mathbf{x}} \in X \cap \Big(\mathbf{H}^2(\Omega)\times H^1(\Omega)\Big),
$$

and

$$
\bar{\mathbf{y}} \in Y \cap \Big(\mathbf{H}^2(\Omega)\times H^1(\Omega)\Big).
$$

4. Sensitivity with respect to the domain

Let us consider a domain $\mathcal{D}$ such that $\mathcal{D} \supset \bar{\Omega}$ and let

$$
\mathcal{T}_{ad} = \{\mathbf{V} \in C^{1,1}(\bar{\mathcal{D}})^2 : \mathbf{V} = 0 \text{ on } \partial\mathcal{D}\cup\Gamma_D\}
$$

be the space of deformation fields. Then the fields $\mathbf{V} \in \mathcal{T}_{ad}$ define for $t > 0$, a perturbation of Ω by means of

$$
\begin{aligned}
T_t : \Omega &\mapsto \Omega_t,\\
x &\mapsto T_t(x) = x + t\mathbf{V}(x).
\end{aligned}
$$

For each $\mathbf{V} \in \mathcal{T}_{ad}$ and t sufficiently small, it can be shown that $\{T_t\}$ is a family of $C^{1,1}$ diffeomorphims [34]. Since $\mathbf{V}$ vanishes on Γ_D for $\mathbf{V} \in \mathcal{T}_{ad}$, it follows that Γ_D is a part of Ω_t for all t.

On the perturbed domain Ω_t, the solutions $(\mathbf{u}_{Dt}, p_{Dt}) := (\mathbf{u}_D(\Omega_t), p_D(\Omega_t))$, and $(\mathbf{u}_{Nt}, p_{Nt}) := (\mathbf{u}_N(\Omega_t), p_N(\Omega_t))$ satisfy

$$
\begin{cases}
-\alpha\Delta\mathbf{u}_{Dt} + \nabla p_{Dt} = \mathbf{f}_t \text{ in } \quad \Omega_t, \\
\operatorname{div} \mathbf{u}_{Dt} = 0 \quad \text{in} \quad \Omega_t, \\
\mathbf{u}_{Dt} = 0 \quad \text{on} \quad \Gamma_D, \\
\mathbf{u}_{Dt} \cdot \mathbf{n}_t = 0, \quad \text{on} \quad \Gamma_{ft}, \\
\alpha \frac{\partial \mathbf{u}_{Dt}}{\partial \mathbf{n}_t} \cdot \boldsymbol{\tau}_t = 0, \quad \text{on} \quad \Gamma_{ft},
\end{cases}
\tag{16}
$$

and

$$
\begin{cases}
-\alpha\Delta\mathbf{u}_{Nt} + \nabla p_{Nt} = \mathbf{f}_t \text{ in } \quad \Omega_t, \\
\operatorname{div} \mathbf{u}_{Nt} = 0 \quad \text{in} \quad \Omega_t, \\
\mathbf{u}_{Nt} = 0 \quad \text{on} \quad \Gamma_D, \\
-p_{Nt}\mathbf{n} + \alpha \frac{\partial \mathbf{u}_{Nt}}{\partial \mathbf{n}_t} = 0 \quad \text{on} \quad \Gamma_{ft},
\end{cases}
\tag{17}
$$

respectively, where $(\mathbf{n}_t, \boldsymbol{\tau}_t)$ are the unit outward normal and tangent vectors to Γ_{ft}. We say that the function $\mathbf{u}(\Omega)$ has a material derivative $\dot{\mathbf{u}}$ at zero in the direction $\mathbf{V}$ if the limit

$$
\dot{\mathbf{u}} = \lim_{t\to 0^+} \frac{\mathbf{u}(\Omega_t) \circ T_t - \mathbf{u}(\Omega)}{t}
\tag{18}
$$

exists, where $(\mathbf{u}(\Omega_t) \circ T_t)(x) = \mathbf{u}(\Omega_t)(T_t(x))$.

The function $\mathbf{u}(\Omega)$ is said to have a shape derivative $\mathbf{u}'$ at zero in the direction $\mathbf{V}$ if the limit

$$
\mathbf{u}' = \lim_{t\to 0^+} \frac{\mathbf{u}(\Omega_t) - \mathbf{u}(\Omega)}{t}
\tag{19}
$$

exists. Moreover, it can be shown that the material and shape derivatives of $\mathbf{u}(\Omega)$ are related by

$$
\dot{\mathbf{u}} = \mathbf{u}' + D\mathbf{u} \cdot \mathbf{V},
$$

provided that $D\mathbf{u} \cdot \mathbf{V}$ exists in some appropriate function space [9, 34].

Definition 4.1. *For given $\mathbf{V} \in \mathcal{T}_{ad}$, the Eulerian derivative of J at Ω in the direction $\mathbf{V}$ is defined as*

$$
dJ(\Omega, V) = \lim_{t\to 0^+} \frac{J(\Omega_t) - J(\Omega)}{t},
\tag{20}
$$

provided that the limit exists. If $dJ(\Omega, \mathbf{V})$ exists for all $V \in \mathcal{T}_{ad}$ and the mapping $\mathbf{V} \mapsto dJ(\Omega, \mathbf{V}$ is linear and continuous on $\mathcal{T}_{ad}$, then we say that $J(\Omega)$ is shape differentiable at Ω and $dJ(\Omega, \cdot)$ is called the shape derivative of $J(\Omega)$ at Ω.

In order to prove the existence of (18), (19), and consequently (20), some useful transformation and differentiation results that are subsequently needed are listed below.

Lemma 4.1. [17, 34], [9, Chapter 7] *Let $\mathcal{J} = [0, \boldsymbol{\tau}_0]$ with $\boldsymbol{\tau}_0$ sufficiently small. Then the following regularity properties of the transformation T_t hold*

$$
\begin{aligned}
&t \mapsto w_t \in C^1(\mathcal{J}, C(\bar{\Gamma})) && t \mapsto T_t \in C^1(\mathcal{J}, C^1(\bar{\mathcal{D}}; \mathbb{R}^2))\\
&t \mapsto T_t^{-1} \in C(\mathcal{J}, C^1(\bar{\mathcal{D}}; \mathbb{R}^2)) && t \mapsto I_t \in C^1(\mathcal{J}, C(\bar{\mathcal{D}}))\\
&t \mapsto B_t \in C(\mathcal{J}, C^1(\bar{\mathcal{D}}; \mathbb{R}^{2\times 2})) && \tfrac{d}{dt} T_t|_{t=0} = \mathbf{V}\\
&\tfrac{d}{dt} T_t^{-1}|_{t=0} = -\mathbf{V} && \tfrac{d}{dt} B_t^{-T}|_{t=0} = D\mathbf{V}\\
&\tfrac{d}{dt} B_t^{T}|_{t=0} = -D\mathbf{V} && \tfrac{d}{dt} I_t|_{t=0} = div\ \mathbf{V}\\
&\tfrac{d}{dt} w_t|_{t=0} = div_\Gamma \mathbf{V} && \tfrac{d}{dt} \mathcal{C}(t)|_{t=0} = div\mathbf{V} + D\mathbf{V}\\
&\tfrac{d}{dt} A(t)|_{t=0} = div\mathbf{V} - (D\mathbf{V} + (D\mathbf{V})^T),
\end{aligned} \tag{21}
$$

where here and in what follows, the following notation is utilized

$$
\begin{aligned}
&I_t := det\ DT_t, \quad B_t := DT_t^{-T}, \quad A(t) := I_t(x) B_t(x)^{-T} B_t, \quad \mathcal{C}(t) := I_t(B_t)\\
&w_t := |I_t B_t \boldsymbol{n}|, \quad A := \frac{d}{dt} A(t)|_{t=0}, \quad \mathcal{C} := \frac{d}{dt} \mathcal{C}(t)|_{t=0},
\end{aligned}
$$

and the limits defining the derivatives at $t = 0$ exist uniformly in $x \in \bar{\mathcal{D}}$.

Lemma 4.2. [17]

(1) *Let $g \in C(\mathcal{J}, W^{1,1}(\mathcal{D}))$, and assume that $\frac{\partial g}{\partial t}(0)$ exists in $L^1(\mathcal{D})$. Then*

$$
\frac{d}{dt} \int_{\Omega_t} g(t,x)\, d\Omega_t|_{t=0} = \int_\Omega \frac{\partial g}{\partial t}(0,x)\, d\Omega + \int_\Gamma g(0,x) \mathbf{V} \cdot \boldsymbol{n}\, d\Gamma.
$$

(2) *Let $g \in C(\mathcal{J}, W^{2,1}(\mathcal{D}))$, and assume that $\frac{\partial g}{\partial t}(0)$ exists in $W^{1,1}(\mathcal{D})$. Then*

$$
\frac{d}{dt} \int_{\Gamma_t} g(t,x)\, d\Omega_t|_{t=0} = \int_\Gamma \frac{\partial g}{\partial t}(0,x)\, d\Gamma + \int_\Gamma \Big(\frac{\partial g(0,x)}{\partial \mathbf{n}} + \kappa g(0,x) \Big) \mathbf{V} \cdot \boldsymbol{n}\, d\Gamma,
$$

where κ stands for the mean curvature of Γ.

For the transformation of domain and boundary integrals, the following well known facts will be used repeatedly.

Lemma 4.3. *Let $\phi_t \in L^1(\Omega_t)$, $\varphi_t \in L^1(\Gamma_t)$, then $\phi_t \circ T_t \in L^1(\Omega)$, $\varphi_t \circ T_t \in L^1(\Gamma)$ and*

$$
\int_{\Omega_t} \phi_t\, d\Omega_t = \int_\Omega (\phi_t \circ T_t) I_t\, d\Omega, \qquad \int_{\Gamma_t} \varphi_t\, d\Gamma_t = \int_\Gamma w_t (\varphi_t \circ T_t)\ d\Gamma.
$$

Lemma 4.4. [16] *For any $f \in L^p(\mathcal{D})$, $p \geq 1$, we have $\lim_{t\to 0} f \circ T_t = f$ in $L^p(\mathcal{D})$.*

4.1. **Existence of shape derivatives.** In this subsection we further assume that the data $\mathbf{f} \in \mathbf{H}^1(\mathcal{D})$ and prove that the mapping $t \mapsto (\mathbf{u}_D^t, p_D^t)$ with values in X is C^1 in the neighborhood of 0. Furthermore, we characterize the shape derivatives $(\mathbf{u}_D', p_D')$ of $(\mathbf{u}_D, p_D)$. Regarding the differentiability of $(\mathbf{u}_N, p_N)$ with respect to Ω, we utilize the following result based on [2, Proposition 2.5].

Theorem 4.1. *Let $\mathbf{f} \in \mathbf{H}^1(\mathcal{D})$ and $\boldsymbol{V} \in \mathcal{T}_{ad}$ be a given vector field. Then the solution $(\boldsymbol{u}_N, p_N) \in Y \cap (\boldsymbol{H}(\Omega)^3 \times H^2(\Omega))$ is differentiable with respect to the domain and the shape derivative $(\boldsymbol{u}_N', p_N') \in Y \cap (\boldsymbol{H}(\Omega)^2 \times H^1(\Omega))$ is the only solution to the boundary value problem*

$$\left\{\begin{array}{l} -\alpha\Delta \boldsymbol{u}_N' + \nabla p_N' = 0 \;\; in \quad \Omega, \\ div\; \boldsymbol{u}_N' = 0 \quad in \quad \Omega, \\ \boldsymbol{u}_N' = 0 \quad on \quad \Gamma_D, \\ -p_N'\boldsymbol{n} + \alpha \frac{\partial \boldsymbol{u}_N'}{\partial \boldsymbol{n}} = \alpha div_\Gamma(\nabla_\Gamma \boldsymbol{u}_N(\boldsymbol{V}\cdot\boldsymbol{n})) + (\boldsymbol{f} - \kappa p_N \boldsymbol{n})\boldsymbol{V}\cdot\boldsymbol{n} - \nabla_\Gamma(p_N \boldsymbol{V}\cdot\boldsymbol{n}) \quad on \quad \Gamma_f. \end{array}\right. \tag{22}$$

Next, we turn to the differentiability of $(\mathbf{u}_D, p_D)$ with respect to Ω. First, observe that on Ω_t, the weak formulation in (14) becomes:
Find $\bar{\mathbf{x}}_t := (\mathbf{u}_{Dt}, p_{Dt}) \in X_t$ such that

$$\begin{array}{r} \langle E_1(\bar{\mathbf{x}}_t, \Omega_t), \Theta_t\rangle_{X_t^*\times X_t} := \alpha(\nabla \mathbf{u}_{Dt}, \nabla \boldsymbol{\psi}_t)_{\Omega_t} - (p_D, \text{div}\; \boldsymbol{\psi}_t)_{\Omega_t} - (\text{div}\; \mathbf{u}_{Dt}, \xi_t)_{\Omega_t} \\ -(\mathbf{f}_t, \boldsymbol{\psi}_t)_{\Omega_t} = 0, \end{array} \tag{23}$$

for all $\Theta_t := (\boldsymbol{\psi}_t, \xi_t) \in X_t$, where $X_t := W(\Omega_t) \times L_0^2(\Omega_t)$.
Mapping (23) back to Ω we obtain the variational formulation:
Find $\bar{\mathbf{x}}^t := (\mathbf{u}_D^t, p_D^t) \in X$ such that

$$\begin{array}{r} \langle \tilde{E}_1(\bar{\mathbf{x}}^t, t), \Theta\rangle_{X^*\times X} := \alpha(A(t)\nabla \mathbf{u}_D^t, \nabla\boldsymbol{\psi})_\Omega - (p_D^t, \mathcal{C}(t) : \nabla\boldsymbol{\psi})_\Omega - (\mathcal{C}(t) : \nabla u^t, \xi)_\Omega \\ -(I_t \mathbf{f}^t, \boldsymbol{\psi})_\Omega = 0, \end{array} \tag{24}$$

for all $\Theta \in X$.

Theorem 4.2. *Let $\bar{\mathbf{x}} := (\boldsymbol{u}_D, p_D) \in X$. Then $\tilde{E}_1 : X \times (-\tilde{\tau}, \tilde{\tau}) \mapsto X^*$ is a C^1-function such that $E_1(\bar{\mathbf{x}}, \Omega) = 0$ is equivalent to $\tilde{E}(\bar{\mathbf{x}}^t, t) = 0$ in X^*, with $\tilde{E}_1(\bar{\mathbf{x}}, 0) = E_1(\bar{\mathbf{x}}, \Omega)$ for all $\bar{\mathbf{x}} \in X$.*

Proof. Observe that since $\mathbf{f} \in \mathbf{H}^1(\Omega)$, and that the coefficients $A(t)$ and $B(t)$ are C^1 by (21), $\tilde{E}_1(\bar{\mathbf{x}}^t, t)$ is a C^1-function in a neighborhood of $(\bar{\mathbf{x}}, 0)$. Moreover, $\tilde{E}_1(\bar{\mathbf{x}}, 0)$=$E_1(\bar{\mathbf{x}}, \Omega)$ by construction. □

Theorem 4.3. *For every $\boldsymbol{f} \in \mathbf{H}^1(\Omega)$ and $\phi \in L_0^2(\Omega)$, the linearized equation*

$$\langle E_{1\bar{\mathbf{x}}}(\bar{\mathbf{x}}, \Omega)(\boldsymbol{v}, \pi), \Theta\rangle_{X^*\times X} = (\boldsymbol{f}, \boldsymbol{\psi})_\Omega + (\phi, \xi)_\Omega, \quad (\boldsymbol{\psi}, \xi) \in X,$$

where

$$\langle E_{1\bar{\mathbf{x}}}(\bar{\mathbf{x}}, \Omega)(\boldsymbol{v}, \pi), \Theta\rangle_{X^*\times X} := \alpha(\nabla \boldsymbol{v}, \nabla\boldsymbol{\psi})_\Omega - (\pi, div\; \boldsymbol{\psi})_\Omega - (div\; \boldsymbol{v}, \xi)_\Omega,$$

has a unique solution $(\boldsymbol{v}, \pi) \in X$, provided that (14) admits a unique solution $\bar{\mathbf{x}}$.

Proof. The operator $E_{1\bar{\mathbf{x}}}(\bar{\mathbf{x}},\Omega)$ is linear and bounded from X into X^*. Hence we have to check whether, for each $\mathbf{f}\in\mathbf{H}^1(\Omega)$ and $\phi\in L^2_0(\Omega)$, there exist a unique solution $(\mathbf{v},\pi)$ to the system

$$(25)\qquad \begin{cases} -\alpha\Delta\mathbf{v}+\nabla\pi=\mathbf{f} \text{ in } \quad \Omega,\\ \operatorname{div}\mathbf{v}=\phi \quad \text{in} \quad \Omega,\\ \mathbf{v}=0 \quad \text{on} \quad \Gamma_D,\\ \mathbf{v}\cdot\mathbf{n}=0, \quad \text{on} \quad \Gamma_f,\\ \alpha\frac{\partial\mathbf{v}}{\partial\mathbf{n}}\cdot\boldsymbol{\tau}=0, \quad \text{on} \quad \Gamma_f, \end{cases}$$

that depends continuously on the data. Since Ω is a domain of class $C^{1,1}$ and $\phi\in L^2_0(\Omega)$, Corollary 2.4 in [12] implies that there exist $\mu\in\mathbf{H}^1_0(\Omega)$ such that $\operatorname{div}\mu=\phi$. Setting $\hat{v}:=\mathbf{v}-\mu$, system (25) becomes

$$(26)\qquad \begin{cases} -\alpha\Delta\hat{v}+\nabla\pi=F \text{ in } \quad \Omega,\\ \operatorname{div}\hat{v}=0 \quad \text{in} \quad \Omega,\\ \hat{v}=0 \quad \text{on} \quad \Gamma_D,\\ \hat{v}\cdot\mathbf{n}=0, \quad \text{on} \quad \Gamma_f,\\ \alpha\frac{\partial\hat{v}}{\partial\mathbf{n}}\cdot\boldsymbol{\tau}=0, \quad \text{on} \quad \Gamma_f, \end{cases}$$

where $F=\mathbf{f}+\alpha\Delta\mu$. Following [26], it easily follows that system (26) possesses a unique solution depending continuously on the data. Hence the operator $\tilde{E}_{1\bar{\mathbf{x}}}(\bar{\mathbf{x}},0)$ is an isomorphism from X onto X^*. ☐

Lemma 4.5. *If Theorems 4.2 and 4.3 hold, then the mapping $(-\tau,\tau)\mapsto X : t\mapsto(\boldsymbol{u}^t_D,p^t_D)$ is differentiable, i.e., there exits $\dot{\mathbf{x}}:=(\dot{\boldsymbol{u}}_D,\dot{p}_D)\in X$ such that*

$$\lim_{t\to 0^+}\|\frac{\boldsymbol{u}^t_D-\boldsymbol{u}_D}{t}-\dot{\mathbf{u}}_D\|_{W(\Omega)}+\lim_{t\to 0^+}\|\frac{p^t_D-p_D}{t}-\dot{p}_D\|_{L^2_0(\Omega)}=0,$$

and $\dot{\mathbf{x}}$ verifies

$$(27)\qquad \langle\tilde{E}_{1t}(\bar{\mathbf{x}},0),\Theta\rangle_{X^*\times X}+\langle\tilde{E}_{1\bar{\mathbf{x}}}(\bar{\mathbf{x}},0)\dot{\mathbf{x}},\Theta\rangle_{X^*\times X}=0,$$

where

$$\begin{aligned}\langle\tilde{E}_{1\bar{\mathbf{x}}}(\bar{\mathbf{x}},0)\dot{\mathbf{x}},\Theta\rangle_{X^*\times X}&:=\alpha(\nabla\dot{\boldsymbol{u}}_D,\nabla\boldsymbol{\psi})_\Omega-(\dot{p}_D,div\ \boldsymbol{\psi})_\Omega-(div\ \dot{\boldsymbol{u}}_D,\xi)_\Omega,\\ \langle\tilde{E}_{1t}(\bar{\mathbf{x}},0),\Theta\rangle_{X^*\times X}&:=\alpha(A\nabla\boldsymbol{u}_D,\nabla\boldsymbol{\psi})_\Omega-(p_D,\mathcal{C}:\nabla\boldsymbol{\psi})_\Omega-(\mathcal{C}:\nabla u,\xi)_\Omega-(div(\boldsymbol{f}\mathbf{V}),\boldsymbol{\psi})_\Omega,\end{aligned}$$

$A:=\partial_t A(t)|_{t=0}$ and $\mathcal{C}:=\partial_t\mathcal{C}(t)|_{t=0}$.

Proof. The unique solution $\bar{\mathbf{x}}$ of $E_1(\bar{\mathbf{x}},\Omega)$ satisfies $E_1(\bar{\mathbf{x}},\Omega)=\tilde{E}_1(\bar{\mathbf{x}},0)=0$ and

$$E_{1\bar{\mathbf{x}}}(\bar{\mathbf{x}},\Omega)=\tilde{E}_{1\bar{\mathbf{x}}}(\bar{\mathbf{x}},0).$$

Since $E_{1\bar{\mathbf{x}}}(\bar{\mathbf{x}},\Omega)$ is bijective by Theorem 4.3, $\tilde{E}_{1\bar{\mathbf{x}}}(\bar{\mathbf{x}},0)$ is also bijective. We now have three Banach spaces X, X^* and $\mathbb{R}$, an open set $X\times(-\tilde{\tau},\tilde{\tau})$ of $X\times\mathbb{R}$, a continuously differentiable function $\tilde{E}_1 : X\times(-\tilde{\tau},\tilde{\tau})\mapsto X^*$ and an element $(\bar{\mathbf{x}},0)\in X\times(-\tilde{\tau},\tilde{\tau})$ such that $\tilde{E}_1(\bar{\mathbf{x}},0)=0$ and $\tilde{E}_{1\bar{\mathbf{x}}}(\bar{\mathbf{x}},0)\in\mathcal{L}(X,X^*)$ is an isomorphism between X and X^*. Hence the generalized implicit function theorem can be applied and one finds that there exist neighborhoods $U \subset X$ and $(-\tau_0, \tau_0) \subset (-\tilde{\tau}, \tilde{\tau})$ of $\bar{\mathbf{x}}$ and 0, respectively, and a differentiable function $g : (-\tau_0, \tau_0) \mapsto U$ such that

$$\tilde{E}_1(g(t), t) = 0 \tag{28}$$

for all $t \in (-\tau_0, \tau_0)$ and moreover, $g(t)$ is the only solution to (24) in U. Let $\bar{\mathbf{x}}^t := g(t) \in U$ for $|t| < \boldsymbol{\tau}_0$. Then $\bar{\mathbf{x}}^t$ satisfies

$$\|\bar{\mathbf{x}}^t - \bar{\mathbf{x}}^0 - \dot{\mathbf{x}}\|_X = \|o(t)\|_X,$$

and the chain rule leads to (27). $\square$

Remark 4.1. *As a consequence of Lemma 4.5, we have*

$$0 \leq \frac{\|\boldsymbol{u}_D^t - \boldsymbol{u}_D\|_{W(\Omega)}}{t^{1/2}} + \frac{\|p_D^t - p_D\|_{L_0^2(\Omega)}}{t^{1/2}} \leq (\|\dot{\mathbf{u}}_D\|_{W(\Omega)} + \|\dot{p}_D\|_{L^2(\Omega)})t^{1/2} + \|\frac{o(t)}{t}\|_X t^{1/2} \tag{29}$$

and

$$\lim_{t\to 0^+} \frac{\|\boldsymbol{u}_D^t - \boldsymbol{u}_D\|_{W(\Omega)}}{t^{1/2}} + \lim_{t\to 0^+} \frac{\|p_D^t - p_D\|_{L_0^2(\Omega)}}{t^{1/2}} = 0. \tag{30}$$

Lemma 4.6. *$\tilde{E}_1$, E_1 and $E_{1\bar{\mathbf{x}}}(\bar{\mathbf{x}}, \Omega) \in \mathcal{L}(X, X^*)$ satisfy*

(i) $\lim\limits_{t\to 0} \frac{1}{t}\langle E_1(\bar{v}, \Omega) - E_1(\bar{\mathbf{x}}, \Omega) - E_{1\bar{\mathbf{x}}}(\bar{\mathbf{x}}, \Omega)(\bar{v} - \bar{\mathbf{x}}), \Theta\rangle_{X^*\times X} = 0,$ *for every $\Theta \in X$ and $\bar{\mathbf{x}}, \bar{v} \in X$.*

(ii) $\lim\limits_{t\to 0} \frac{1}{t}\langle \tilde{E}_1(\bar{\mathbf{x}}^t, t) - \tilde{E}_1(\bar{\mathbf{x}}, t) - \Big(E_1(\bar{\mathbf{x}}^t, \Omega) - E_1(\bar{\mathbf{x}}, \Omega)\Big), \Theta\rangle_{X^*\times X} = 0,$ *for every $\Theta \in X$, where $\bar{\mathbf{x}}^t$ and $\bar{\mathbf{x}}$ are solutions of (24) and (14), respectively.*

Proof. The first statement follows from the linearity of E_1. Let us now verify the second statement. Let $T := \langle \tilde{E}_1(\bar{\mathbf{x}}^t, t) - \tilde{E}_1(\bar{\mathbf{x}}, t) - \Big(E_1(\bar{\mathbf{x}}^t, \Omega) - E_1(\bar{\mathbf{x}}, \Omega)\Big), \Theta\rangle_{X^*\times X}$. Then we can express T as

$$\begin{aligned} T = \int_\Omega \Big\{ &\alpha(A(t) - I)\nabla(\mathbf{u}_D^t - \mathbf{u}_D) : \nabla\boldsymbol{\psi} - (p_D^t - p_D)(\mathcal{C}(t) - I) : \nabla\boldsymbol{\psi} \\ &- (\mathcal{C}(t) - I) : \nabla(\mathbf{u}_D^t - \mathbf{u}_D)\xi \Big\}\, d\Omega, \end{aligned}$$

and the estimate

$$\begin{aligned} |T| \leq\ &\|(A(t) - I)\|_{L^\infty(\Omega)}\|\mathbf{u}_D^t - \mathbf{u}_D\|_{W(\Omega)}\|\boldsymbol{\psi}\|_{W(\Omega)} + \|p_D^t - p_D\|_{L_0^2(\Omega)}\|\mathcal{C}(t) - I\|_{L^\infty(\Omega)}\|\boldsymbol{\psi}\|_{W(\Omega)} \\ &+ \|\mathcal{C}(t) - I\|_{L^\infty(\Omega)}\|\mathbf{u}_D^t - \mathbf{u}_D\|_{W(\Omega)}\|\xi\|_{L_0^2(\Omega)}, \end{aligned}$$

holds. Utilizing Remark 4.1 and (21), we obtain the desired result. $\square$

The following lemmas are needed in what follows.

Lemma 4.7. [10] *Let $\boldsymbol{n}$ be an outward norm vector to Γ_f and $\boldsymbol{V} \in \mathcal{T}_{ad}$. Then the shape derivative of $\boldsymbol{n}$ denoted as $\boldsymbol{n}'$ satisfies*

$$\boldsymbol{n}' = -\nabla_{\Gamma_f}(\boldsymbol{V} \cdot \boldsymbol{n}).$$

Lemma 4.8. *Let $\boldsymbol{n}$ be an outward norm vector to Γ. Then*

$$\frac{\partial(\boldsymbol{u} \cdot \boldsymbol{n})}{\partial \boldsymbol{n}} = \frac{\partial \boldsymbol{u}}{\partial \boldsymbol{n}}\boldsymbol{n}. \tag{31}$$

Proof. Since $\mathbf{n}^2 = 1$, we take the derivatives on both side of this equation to obtain $D\mathbf{n}\cdot\mathbf{n} = 0$. Utilizing this result, and taking derivatives on both sides of (31), gives the desired result. ☐

Lemma 4.9. [10] *The shape derivative of the slip boundary condition* $\boldsymbol{u}\cdot\boldsymbol{n} = 0$ *on* Γ_f *is given by*

$$\boldsymbol{u}'\cdot\boldsymbol{n} = div_\Gamma(\boldsymbol{u}\boldsymbol{V}\cdot\boldsymbol{n}) \quad on \quad \Gamma_f.$$

Lemma 4.10. *Let* $\boldsymbol{\psi}\in W(\Omega)\cap\mathbf{H}^2(\Omega)$ *and* $\boldsymbol{V}\in\mathcal{T}_{ad}$. *Then*

$$\hat{\boldsymbol{\psi}}\cdot\boldsymbol{n} = \boldsymbol{\psi}\cdot\nabla_\Gamma(\boldsymbol{V}\cdot\boldsymbol{n}) + (div_\Gamma\ \boldsymbol{\psi} - div\ \boldsymbol{\psi})\boldsymbol{V}\cdot\boldsymbol{n}, \tag{32}$$

where $\hat{\boldsymbol{\psi}} := -\nabla\boldsymbol{\psi}\cdot\boldsymbol{V}\in\mathbf{H}^1(\Omega)$.

Proof. Note that

$$\hat{\boldsymbol{\psi}}\cdot\mathbf{n} = -\langle\mathbf{V}, D_\Gamma\boldsymbol{\psi}^T\mathbf{n}\rangle - \langle D\boldsymbol{\psi}\cdot\mathbf{n},\mathbf{n}\rangle\mathbf{V}\cdot\mathbf{n}. \tag{33}$$

Lemma 5.1 in [10] implies that

$$(D_\Gamma\boldsymbol{\psi})^T\mathbf{n} = -(D_\Gamma\mathbf{n})^T\boldsymbol{\psi} + \nabla_\Gamma(\boldsymbol{\psi}\cdot\mathbf{n}) \tag{34}$$

$$(D_\Gamma\mathbf{n})^T\mathbf{V} = -(D_\Gamma\mathbf{V})^T\mathbf{n} + \nabla_\Gamma(\mathbf{V}\cdot\mathbf{n}). \tag{35}$$

Since $\boldsymbol{\psi}\in W(\Omega)$ and that $(D_\Gamma\mathbf{n})^T = (D_\Gamma\mathbf{n})$ [10], we have that

$$\begin{aligned}\hat{\boldsymbol{\psi}}\cdot\mathbf{n} &= \langle(D_\Gamma\mathbf{n})^T\mathbf{V},\boldsymbol{\psi}\rangle - \langle D\boldsymbol{\psi}\cdot\mathbf{n},\mathbf{n}\rangle\mathbf{V}\cdot\mathbf{n},\\ &= \langle\nabla_\Gamma(\mathbf{V}\cdot\mathbf{n}),\boldsymbol{\psi}\rangle - \langle D\boldsymbol{\psi}\cdot\mathbf{n},\mathbf{n}\rangle\mathbf{V}\cdot\mathbf{n} - \langle(D_\Gamma\mathbf{V})^T\mathbf{n},\boldsymbol{\psi}\rangle.\end{aligned} \tag{36}$$

The last term in (36) vanishes for perturbation fields $\mathbf{V}$ in the normal direction, and replacing $-\langle D\boldsymbol{\psi}\cdot\mathbf{n},\mathbf{n}\rangle\mathbf{V}\cdot\mathbf{n}$ by $(\mathrm{div}_\Gamma\ \boldsymbol{\psi} - \mathrm{div}\ \boldsymbol{\psi})\mathbf{V}\cdot\mathbf{n}$, we obtain the desired result. ☐

Remark 4.2. *If* $div\ \boldsymbol{\psi} = 0$, *then it follows from Lemma 4.10 that* $\hat{\boldsymbol{\psi}}\cdot\boldsymbol{n} = div_\Gamma(\boldsymbol{\psi}(\boldsymbol{V}\cdot\boldsymbol{n}))$ *on* Γ_f.

Proposition 4.1. *The solution* $(\boldsymbol{u}_D, p_D)\in X\cap(\boldsymbol{H}^2(\Omega)\times H^1(\Omega))$ *is differentiable with respect to the domain and its shape derivative* $(\boldsymbol{u}_D', p_D')\in\boldsymbol{H}^1(\Omega)\times L^2_0(\Omega)$ *is the only solution to the boundary value problem*

$$\begin{cases} -\alpha\Delta\boldsymbol{u}_D' + \nabla p_D' = 0 \ in \quad \Omega,\\ div\ \boldsymbol{u}_D' = 0 \quad in \quad \Omega,\\ \boldsymbol{u}_D' = 0 \quad on \quad \Gamma_D,\\ \boldsymbol{u}_D'\cdot\boldsymbol{n} = div_\Gamma(\boldsymbol{u}_D(\boldsymbol{V}\cdot\boldsymbol{n})), \quad on \quad \Gamma_f,\end{cases} \tag{37}$$

and

$$\int_{\Gamma_f}\sigma_{\boldsymbol{\tau}}(\boldsymbol{u}_D', p_D')\boldsymbol{\psi}\cdot\boldsymbol{\tau}\, d\Gamma = \int_{\Gamma_f}\left\{-\sigma_{nn}\hat{\boldsymbol{\psi}}\cdot\boldsymbol{n} - [\alpha\nabla\boldsymbol{u}_D\cdot\nabla\boldsymbol{\psi} - p_D\ div\ \boldsymbol{\psi} - \mathbf{f}\cdot\boldsymbol{\psi}]\boldsymbol{V}\cdot\boldsymbol{n}\right\} d\Gamma, \tag{38}$$

for all $\boldsymbol{\psi}\in W(\Omega)\cap\mathbf{H}^2(\Omega)$, *where* $\hat{\boldsymbol{\psi}}\cdot\boldsymbol{n} = -\langle\boldsymbol{V}, D_\Gamma\boldsymbol{\psi}^T\boldsymbol{n}\rangle - \langle D\boldsymbol{\psi}\cdot\boldsymbol{n},\boldsymbol{n}\rangle\boldsymbol{V}\cdot\boldsymbol{n}$, $\sigma(\mathbf{v},q)\cdot\mathbf{n} := -q\mathbf{n} + \alpha\frac{\partial\mathbf{v}}{\partial\mathbf{n}}$, $\sigma_{\boldsymbol{nn}} := \sigma(\boldsymbol{u}_D, p_D)\cdot\boldsymbol{n}\cdot\boldsymbol{n}$, $\sigma_{\boldsymbol{\tau}}(\boldsymbol{u}_D', p_D') := (\sigma(\boldsymbol{u}_D', p_D')\cdot\boldsymbol{n})\cdot\boldsymbol{\tau}$ *and* $\boldsymbol{\tau}$ *is the unit tangent vector to* Γ_f.

Proof. Lemma 4.5 implies

$$\langle \tilde{E}_{1\bar{\mathbf{x}}}(\bar{\mathbf{x}},0)\dot{\mathbf{x}},\Theta\rangle_{X^*\times X}. = -\langle \tilde{E}_{1t}(\bar{\mathbf{x}},0),\Theta\rangle_{X^*\times X}. \tag{39}$$

Following [17], we can express $\langle \tilde{E}_{1\bar{\mathbf{x}}}(\bar{\mathbf{x}},0)(\bar{\mathbf{x}}^t-\bar{\mathbf{x}}),\Theta\rangle_{X^*\times X}$ as

$$\begin{aligned}\langle \tilde{E}_{1\bar{\mathbf{x}}}(\bar{\mathbf{x}},0)(\bar{\mathbf{x}}^t-\bar{\mathbf{x}}),\Theta\rangle_{X^*\times X} &= -\langle \tilde{E}_1(\bar{\mathbf{x}},t)-\tilde{E}_1(\bar{\mathbf{x}},0),\Theta\rangle_{X^*\times X}\\ &\quad -\langle E_1(\bar{\mathbf{x}}^t,\Omega)-E_1(\bar{\mathbf{x}},\Omega)-E_{1\bar{\mathbf{x}}}(\bar{\mathbf{x}},\Omega)(\bar{\mathbf{x}}^t-\bar{\mathbf{x}}),\Theta\rangle_{X^*\times X}\\ &\quad -\langle \tilde{E}_1(\bar{\mathbf{x}}^t,t)-\tilde{E}_1(\bar{\mathbf{x}},t)-E_1(\bar{\mathbf{x}}^t,\Omega)+E_1(\bar{\mathbf{x}},\Omega),\Theta\rangle_{X^*\times X}.\end{aligned}$$

Utilizing Lemma 4.6, we find that

$$\langle \tilde{E}_{1\bar{\mathbf{x}}}(\bar{\mathbf{x}},0)\dot{\mathbf{x}},\Theta\rangle_{X^*\times X} = -\frac{d}{dt}\langle \tilde{E}_1(\bar{\mathbf{x}},t),\Theta\rangle_{X^*\times X}|_{t=0}, \tag{40}$$

where $\langle \tilde{E}_1(\bar{\mathbf{x}},t),\Theta\rangle_{X^*\times X}$ can expressed as

$$\begin{aligned}\langle \tilde{E}_1(\bar{\mathbf{x}},t),\Theta\rangle_{X^*\times X} &:= (\alpha\nabla(\mathbf{u}_D\circ T_t^{-1}),\nabla(\boldsymbol{\psi}\circ T_t^{-1}))_{\Omega_t}-(p_D\circ T_t^{-1},\text{div }(\boldsymbol{\psi}\circ T_t^{-1}))_{\Omega_t}\\ &\quad -(\mathbf{f},\boldsymbol{\psi}\circ T_t^{-1})_{\Omega_t}-(\text{div }(\mathbf{u}_D\circ T_t^{-1}),\xi\circ T_t^{-1})_{\Omega_t}=0.\end{aligned} \tag{41}$$

Utilizing Lemma (4.2), we find

$$\begin{aligned}\frac{d}{dt}\langle \tilde{E}_1(\bar{\mathbf{x}},t),\Theta\rangle_{X^*\times X}|_{t=0} &= \alpha(\nabla\hat{u}_D,\nabla\boldsymbol{\psi})_\Omega+\alpha(\nabla\mathbf{u}_D,\nabla\hat{\boldsymbol{\psi}})_\Omega+\alpha\int_{\Gamma_f}\nabla\mathbf{u}_D\cdot\nabla\boldsymbol{\psi}\,\mathbf{V}\cdot\mathbf{n}\,d\Gamma\\ &\quad -(\hat{p}_D,\text{div }\boldsymbol{\psi})_\Omega-(p_D,\text{div }\hat{\boldsymbol{\psi}})_\Omega-\int_{\Gamma_f}p_D\text{ div }\boldsymbol{\psi}\,\mathbf{V}\cdot\mathbf{n}\,d\Gamma\\ &\quad -(\mathbf{f},\hat{\boldsymbol{\psi}})_\Omega-(\text{div }\hat{u}_D,\xi)_\Omega-\int_{\Gamma_f}\mathbf{f}\cdot\boldsymbol{\psi}\,\mathbf{V}\cdot\mathbf{n}\,d\Gamma,\end{aligned}$$

where $\hat{u}_D := -\nabla\mathbf{u}_D\cdot\mathbf{V}\in\mathbf{H}^1(\Omega)$, $\hat{\boldsymbol{\psi}} := -\nabla\boldsymbol{\psi}\cdot\mathbf{V}\in\mathbf{H}^1(\Omega)$, and $\hat{p}_D := -\nabla p_D\cdot\mathbf{V}\in L^2(\Omega)$.

Since $\dot{\mathbf{x}} = \bar{\mathbf{x}}'+\nabla\bar{\mathbf{x}}\cdot\mathbf{V}$, it follows from (27) and (40) that

$$\begin{aligned}\alpha(\nabla\mathbf{u}_D',\nabla\boldsymbol{\psi})_\Omega-(p_D',\text{div }\boldsymbol{\psi})_\Omega-(\text{div }\mathbf{u}_D',\xi)_\Omega &= -\alpha(\nabla\mathbf{u}_D,\nabla\hat{\boldsymbol{\psi}})_\Omega+(p_D,\text{div }\hat{\boldsymbol{\psi}})_\Omega\\ &\quad +(\mathbf{f},\hat{\boldsymbol{\psi}})_\Omega-\int_{\Gamma_f}[\alpha\nabla\mathbf{u}_D\cdot\nabla\boldsymbol{\psi}-p_D\text{ div }\boldsymbol{\psi}-\mathbf{f}\cdot\boldsymbol{\psi}]\,\mathbf{V}\cdot\mathbf{n}\,d\Gamma.\end{aligned} \tag{42}$$

Integrating by parts the first two terms on the right hand side of (42) and utilizing (9), we find

$$\begin{aligned}\alpha(\nabla\mathbf{u}_D',\nabla\boldsymbol{\psi})_\Omega-(p_D',\text{div }\boldsymbol{\psi})_\Omega-(\text{div }\mathbf{u}_D',\xi)_\Omega &= \int_{\Gamma_f}(-\alpha\frac{\partial\mathbf{u}_D}{\partial\mathbf{n}}+p_D\mathbf{n})\hat{\boldsymbol{\psi}}\,d\Gamma\\ &\quad -\int_{\Gamma_f}[\alpha\nabla\mathbf{u}_D\cdot\nabla\boldsymbol{\psi}-p_D\text{ div }\boldsymbol{\psi}-\mathbf{f}\cdot\boldsymbol{\psi}]\,\mathbf{V}\cdot\mathbf{n}\,d\Gamma.\end{aligned} \tag{43}$$

Choosing $\boldsymbol{\psi}\in\mathcal{D}(\Omega)^2$ and $\xi\in\mathcal{D}(\Omega)$ shows that

$$-\alpha\Delta\mathbf{u}_D'+\nabla p_D' = 0 \text{ in } \quad \Omega, \tag{44}$$

$$\text{div }\mathbf{u}_D' = \text{ in } \quad \Omega, \tag{45}$$

is satisfied in the distributional sense. Since $\mathbf{V} \in \mathcal{T}_{ad}$, the boundary condition satisfied by $\mathbf{u}'_D$ on Γ_D easily follows. On the other-hand, the boundary condition satisfied by $\mathbf{u}'_D \cdot \mathbf{n}$ on Γ_f follows from Lemma 4.9. Next, we verify (4.1).

Applying Greens theorem on both terms on the left hand side of (43), one finds

$$\alpha(\nabla \mathbf{u}'_D, \nabla \boldsymbol{\psi})_\Omega - (p'_D, \operatorname{div} \boldsymbol{\psi})_\Omega = (-\alpha \Delta \mathbf{u}'_D + \nabla p'_D, \boldsymbol{\psi})_\Omega + \int_{\Gamma_f} (\alpha \frac{\partial \mathbf{u}'_D}{\partial \mathbf{n}} - p'_D \mathbf{n}) \boldsymbol{\psi} \, d\Gamma \tag{46}$$

which entails

$$\int_{\Gamma_f} \sigma(\mathbf{u}'_D, p'_D) \cdot \mathbf{n} \boldsymbol{\psi} \, d\Gamma = \int_{\Gamma_f} -\sigma_{nn} \hat{\boldsymbol{\psi}} \cdot \mathbf{n} - [\alpha \nabla \mathbf{u}_D \cdot \nabla \boldsymbol{\psi} - p_D \operatorname{div} \boldsymbol{\psi} - \mathbf{f} \cdot \boldsymbol{\psi}] \, \mathbf{V} \cdot \mathbf{n} \, d\Gamma. \tag{47}$$

Since $\boldsymbol{\psi} \in W$, utilizing Lemma 4.10 in (47) gives the desired result. □

In the rest of the paper, in order to simplify the expressions, we use the following notations

$$\mathbf{w} := \mathbf{u}_D - \mathbf{u}_N, \quad q := p_D - p_N, \quad \mathbf{w}' = \mathbf{u}'_D - \mathbf{u}'_N \quad \text{and} \quad q' = p'_D - p'_N,$$

where $(\mathbf{u}'_D, p'_D)$ and $(\mathbf{u}'_N, p'_N)$ solve (37) and (22), respectively. Moreover, $(\mathbf{w}, q) \in \mathbf{H}^2(\Omega) \cap H^1(\Omega)$ satisfy

$$-\alpha \Delta \mathbf{w} + \nabla q = 0 \quad \text{in } \Omega, \tag{48}$$

$$\operatorname{div} \mathbf{w} = 0 \quad \text{in } \Omega, \tag{49}$$

$$\mathbf{w} = 0 \quad \text{on } \Gamma_D, \tag{50}$$

$$\alpha \frac{\partial \mathbf{w}}{\partial \mathbf{n}} \cdot \boldsymbol{\tau} = 0 \quad \text{on } \Gamma_f. \tag{51}$$

4.2. **Shape derivatives of cost functionals.** The goal here is to derive the shape derivatives of cost functionals $J_i(\Omega)$, $i = 1, \ldots, 3$, in the direction of the deformation field $\mathbf{V}$

4.2.1. *Shape derivative of J_1.*

Proposition 4.2. *Let $\boldsymbol{f} \in \boldsymbol{H}^1(\Omega)$ and $\boldsymbol{V} \in \mathcal{T}_{ad}$. Then the shape functional J_1 is shape differentiable with*

$$dJ_1(\Omega, \boldsymbol{V}) = \int_{\Gamma_f} \Big(\frac{\alpha}{2} |\nabla \boldsymbol{w}|^2 + \alpha \nabla \boldsymbol{u}_N \nabla \boldsymbol{w} - \boldsymbol{f} \boldsymbol{w} - \boldsymbol{u}_D \nabla_\Gamma (-q + \alpha \frac{\partial \boldsymbol{w}}{\partial \boldsymbol{n}} \boldsymbol{n}) \Big) \boldsymbol{V} \cdot \boldsymbol{n} \, d\Gamma.$$

Proof. Since $\mathbf{w} \in \mathbf{H}^2(\Omega)$, $\nabla^2 \mathbf{w} \in L^2(\Omega; \mathbb{R}^{2\times 2})$ and $\nabla \mathbf{w} \in L^2(\Omega; \mathbb{R}^{2\times 2})$, we infer that $|\nabla \mathbf{w}|^2 \in W^{1,1}(\Omega)$ and Lemma 4.2 implies that

$$\begin{aligned} dJ_1(\Omega, \mathbf{V}) &= \int_\Omega \alpha \nabla \mathbf{w} \nabla (\mathbf{u}'_D - \mathbf{u}'_N) + \frac{\alpha}{2} \int_{\Gamma_f} |\nabla \mathbf{w}|^2 \mathbf{V} \cdot \mathbf{n} \, d\Gamma, \\ &= \int_\Omega \alpha \nabla \mathbf{w} \nabla \mathbf{u}'_D \, d\Omega - \int_\Omega \alpha \nabla \mathbf{w} \nabla \mathbf{u}'_N \, d\Omega + \frac{\alpha}{2} \int_{\Gamma_f} |\nabla \mathbf{w}|^2 \mathbf{V} \cdot \mathbf{n} \, d\Gamma. \end{aligned} \tag{52}$$

Applying Green's formula on the first integral in (52), we obtain

$$\int_\Omega \alpha \nabla \mathbf{w} \nabla \mathbf{u}'_D \, d\Omega = -\int_\Omega \alpha \Delta \mathbf{w} \mathbf{u}'_D \, d\Omega + \int_{\Gamma_f} \alpha \frac{\partial \mathbf{w}}{\partial \mathbf{n}} \mathbf{u}'_D \, d\Gamma. \tag{53}$$

Utilizing (48) in the first term on the right hand side of (53) and integrating by parts, we obtain

$$\begin{aligned}\int_\Omega \alpha\nabla\mathbf{w}\nabla\mathbf{u}'_D\, d\Omega &= -\int_\Omega \nabla q\mathbf{u}'_D\, d\Omega + \int_{\Gamma_f} \alpha\frac{\partial\mathbf{w}}{\partial\mathbf{n}}\mathbf{u}'_D\, d\Gamma\\ &= \int_\Omega q \text{ div } \mathbf{u}'_D\, d\Omega + \int_{\Gamma_f} (-q\mathbf{n} + \alpha\frac{\partial\mathbf{w}}{\partial\mathbf{n}})\mathbf{u}'_D\, d\Gamma.\end{aligned}$$

Using system (37) and (51), we find

$$\begin{aligned}\int_\Omega \alpha\nabla\mathbf{w}\nabla\mathbf{u}'_D\, d\Omega &= \int_{\Gamma_f} (-q + \alpha\frac{\partial\mathbf{w}}{\partial\mathbf{n}}\mathbf{n})\mathbf{u}'_D\cdot\mathbf{n}\, d\Gamma,\\ &= \int_{\Gamma_f} (-q + \alpha\frac{\partial\mathbf{w}}{\partial\mathbf{n}}\mathbf{n})\text{div}_\Gamma(\mathbf{u}_D(\mathbf{V}\cdot\mathbf{n}))\, d\Gamma. \end{aligned}\tag{54}$$

Since $\mathbf{u}_D\cdot\mathbf{n} = 0$ on Γ_f, applying the tangential Green's formula (see Section 5.5 in [9]) in (54) gives

$$\int_\Omega \alpha\nabla\mathbf{w}\nabla\mathbf{u}'_D\, d\Omega = \int_{\Gamma_f} -\mathbf{u}_D\nabla_\Gamma(-q + \alpha\frac{\partial\mathbf{w}}{\partial\mathbf{n}}\mathbf{n})\mathbf{V}\cdot\mathbf{n}\, d\Gamma.$$

Analogously, we obtain for the second integral in (37)

$$\begin{aligned}\int_\Omega \alpha\nabla\mathbf{w}\nabla\mathbf{u}'_N\, d\Omega &= -\int_\Omega \alpha\Delta\mathbf{u}'_N\mathbf{w}\, d\Omega + \int_{\Gamma_f} \alpha\frac{\partial\mathbf{u}'_N}{\partial\mathbf{n}}\mathbf{w}\, d\Gamma\\ &= -\int_\Omega \nabla p'_N\mathbf{w}\, d\Omega + \int_{\Gamma_f} \alpha\frac{\partial\mathbf{u}'_N}{\partial\mathbf{n}}\mathbf{w}\, d\Gamma\\ &= \int_\Omega p'_N \text{ div } \mathbf{w}\, d\Omega + \int_{\Gamma_f} (-p'_N\mathbf{n} + \alpha\frac{\partial\mathbf{u}'_N}{\partial\mathbf{n}})\mathbf{w}\, d\Gamma.\end{aligned}$$

Utilizing (49) and (22), we obtain

$$\begin{aligned}\int_\Omega \alpha\nabla\mathbf{w}\nabla\mathbf{u}'_N\, d\Omega &= \int_{\Gamma_f} (-p'_N\mathbf{n} + \alpha\frac{\partial\mathbf{u}'_N}{\partial\mathbf{n}})\mathbf{w}\, d\Gamma,\\ &= \int_{\Gamma_f} (\mathbf{f}\mathbf{w} - \alpha\nabla\mathbf{u}_N\nabla\mathbf{w})\ \mathbf{V}\cdot\mathbf{n}\, d\Gamma.\end{aligned}$$

Summarizing, we find

$$dJ_1(\Omega,\mathbf{V}) = \int_{\Gamma_f} \Big(\frac{\alpha}{2}|\nabla\mathbf{w}|^2 + \alpha\nabla\mathbf{u}_N\nabla\mathbf{w} - \mathbf{f}\mathbf{w} - \mathbf{u}_D\nabla_\Gamma(-q + \alpha\frac{\partial\mathbf{w}}{\partial\mathbf{n}}\mathbf{n})\Big)\mathbf{V}\cdot\mathbf{n}\, d\Gamma.$$

$\square$

4.2.2. *Shape derivative of J_2.* To obtain an expression for the shape derivative of J_2, the adjoint state corresponding equations associated to (10) are needed. To this end we have the following proposition.

Proposition 4.3. *Let $\mathcal{V} := \boldsymbol{u}_N \cdot \boldsymbol{n}$. Then for any $\boldsymbol{u}_N \in Y$, $J_2(\Omega)$ differentiable in the direction $\delta\boldsymbol{u}_N \in Y$ and its directional derivative $J_2'(\Omega)\delta\boldsymbol{u}_N$ is given by*

$$J_2'(\Omega)\delta\boldsymbol{u}_N = \int_{\Gamma_f} \mathcal{V}\delta\boldsymbol{u}_N \cdot \boldsymbol{n}\, d\Gamma. \tag{55}$$

Proof. The proof follows from the definition of a directional derivative of a functional. □

Lemma 4.11. *Let $\bar{\mathbf{y}} := (\boldsymbol{u}_N, p_N) \in Y$, $\Psi := (\boldsymbol{\varphi}, \zeta) \in Y$ and $\mathbf{s} := (\mathbf{z}_N, \pi_N) \in Y$. Then the operator $E_{2\bar{\mathbf{y}}}(\bar{\mathbf{y}}, \Omega)\Psi \in \mathcal{L}(Y, Y^*)$ where*

$$\langle E_{2\bar{\mathbf{y}}}(\bar{\mathbf{y}}, \Omega)\Psi, \mathbf{s}\rangle_{X^*\times X} := \alpha(\nabla\boldsymbol{\varphi}, \nabla\mathbf{z}_N)_\Omega - (\zeta, div\ \mathbf{z}_N)_\Omega - (div\ \boldsymbol{\varphi}, \pi_N)_\Omega, \tag{56}$$

is bijective.

Proof. The operator $E_{2\bar{\mathbf{y}}}(\bar{\mathbf{y}}, \Omega)\Psi$ is bijective if and only if for every $\mathbf{f} \in Y^*$ and $r \in L_0^2(\Omega)$, there exists a unique solution $\bar{\lambda}_N$ to

$$\begin{aligned} -\alpha\Delta\mathbf{z}_N + \nabla\pi_N = \mathbf{f}, &\quad \text{in } \Omega,\\ \text{div } \mathbf{z}_N = r, &\quad \text{in } \Omega,\\ \mathbf{z}_N = 0, &\quad \text{on } \Gamma_D,\\ [-\pi_N\mathbf{n} + \alpha\nabla\mathbf{z}_N \cdot \mathbf{n}] = 0 &\quad \text{on } \Gamma_f. \end{aligned} \tag{57}$$

The existence of a unique solution to (57) is established for instance in [4]. □

As a consequence of Lemma 4.11, there exists a unique adjoint state $\bar{\lambda}_N := (\mathbf{v}_N, q_N) \in Y$ satisfying

$$\langle E_{2\bar{\mathbf{y}}}(\bar{\mathbf{y}}, \Omega)\Psi, \bar{\lambda}_N\rangle_{X^*\times X} = \int_{\Gamma_f} \mathcal{V}\delta\mathbf{u}_N \cdot \mathbf{n}\, d\Gamma, \tag{58}$$

which upon integration by parts amounts to

$$\begin{aligned} -\alpha\Delta\mathbf{v}_N + \nabla q_N = 0, &\quad \text{in } \Omega,\\ \text{div } \mathbf{v}_N = 0, &\quad \text{in } \Omega,\\ \mathbf{v}_N = 0, &\quad \text{on } \Gamma_D,\\ [-q_N\mathbf{n} + \alpha\nabla\mathbf{v}_N \cdot \mathbf{n}] = (\mathbf{u}\cdot\mathbf{n})\mathbf{n} &\quad \text{on } \Gamma_f. \end{aligned} \tag{59}$$

Proposition 4.4. *Let $\boldsymbol{f} \in \boldsymbol{H}^1(\Omega)$ and $\boldsymbol{V} \in \mathcal{T}_{ad}$. Then the shape functional J_2 is shape differentiable with*

$$dJ_2(\Omega, \boldsymbol{V}) = \int_{\Gamma_f} [\boldsymbol{f}\boldsymbol{v}_N - \alpha\nabla\boldsymbol{u}_N : \nabla\boldsymbol{v}_N + div_{\Gamma_f}(\mathcal{V}\boldsymbol{u}_N) + \mathcal{V}(\boldsymbol{n}\frac{\partial\boldsymbol{u}_N}{\partial\boldsymbol{n}} - \kappa\frac{1}{2}\mathcal{V})]\boldsymbol{V}\cdot\boldsymbol{n}\, d\Gamma,$$

where all expressions are evaluated on Γ_f and the adjoint state $\boldsymbol{v}_N$ satisfies (59).

Proof. Since $J_2(\Omega)$ is differentiable with respect to $\mathbf{u}$, by Lemma 4.2 we obtain the Eulerian derivative of $J_2(\Omega)$ with respect to Ω:

$$dJ_2(\Omega,\mathbf{V}) = \int_{\Gamma_f} \mathcal{V}\mathcal{V}' + (\mathcal{V}\frac{\partial \mathcal{V}}{\partial \mathbf{n}} + \kappa\frac{1}{2}\mathcal{V}^2)\mathbf{V}\cdot\mathbf{n}\; d\Gamma, \tag{60}$$

where $\mathcal{V} := \mathbf{u}\cdot\mathbf{n}$ and $\mathcal{V}' = \mathbf{u}'\cdot\mathbf{n} + \mathbf{u}\cdot\mathbf{n}'$. Utilizing Lemma 4.7 and Lemma 4.8, we find that

$$dJ_2(\Omega,\mathbf{V}) = \int_{\Gamma_f} \mathcal{V}\Big(\mathbf{u}_N'\cdot\mathbf{n} - \mathbf{u}_N\nabla_{\Gamma_f}(\mathbf{V}\cdot\mathbf{n}) + (\mathbf{n}\frac{\partial \mathbf{u}_N}{\partial \mathbf{n}} + \kappa\frac{1}{2}\mathcal{V})\mathbf{V}\cdot\mathbf{n}\Big)\, d\Gamma. \tag{61}$$

Testing system (22) with the adjoint variable $(\mathbf{v}_N, q_N)$ and utilizing the adjoint system (59), we obtain

$$0 \;=\; \int_\Omega \Big(\Big(-\alpha\Delta\mathbf{u}_N' + \nabla p_N'\Big)\cdot\mathbf{v}_N - (\mathrm{div}\;\mathbf{u}_N')\cdot q_N\Big)\, d\Omega. \tag{62}$$

Applying Greens formula to equation (62) gives

$$\begin{aligned} 0 \;=\; & \int_\Omega \Big[\Big(-\alpha\Delta\mathbf{v}_N + \nabla q_N\Big)\cdot\mathbf{u}_N' - (\mathrm{div}\;\mathbf{v}_N)\cdot p_N'\Big]\, d\Omega \\ & + \int_{\Gamma_f} \mathbf{u}_N'\Big(-q_N\mathbf{n} + \alpha\frac{\partial \mathbf{v}_N}{\partial \mathbf{n}}\Big)\, d\Gamma - \int_{\Gamma_f}\Big(-p_N'\mathbf{n} + \alpha\frac{\partial \mathbf{u}_N'}{\partial \mathbf{n}}\Big)\mathbf{v}_N\; d\Gamma. \end{aligned} \tag{63}$$

Since $(\mathbf{v}_N, q_N)$ and $(\mathbf{u}_N', p_N')$ satisfy (59) and (22), respectively, we have

$$\begin{aligned} \int_{\Gamma_f}\Big(-p_N'\mathbf{n} + \alpha\frac{\partial \mathbf{u}_N'}{\partial \mathbf{n}}\Big)\mathbf{v}_N\; d\Gamma &= \int_{\Gamma_f} \mathbf{u}_N'\Big(-q_N\mathbf{n} + \alpha\frac{\partial \mathbf{v}_N}{\partial \mathbf{n}}\Big)\, d\Gamma, \\ &= \int_{\Gamma_f} (\mathbf{u}_N'\cdot\mathbf{n})(\mathbf{u}_N\cdot\mathbf{n})\; d\Gamma. \end{aligned} \tag{64}$$

But from (22) and (59), we have that

$$(\alpha\frac{\partial \mathbf{u}_N'}{\partial \mathbf{n}} - p'\mathbf{n}, \mathbf{v}_N)_{\Gamma_f} = \int_{\Gamma_f} [-\alpha\nabla\mathbf{u}_N : \nabla\mathbf{v}_N + \mathbf{f}\mathbf{v}_N]\mathbf{V}\cdot\mathbf{n}\; d\Gamma,$$

and hence

$$\int_{\Gamma_f} (\mathbf{u}_N'\cdot\mathbf{n})(\mathbf{u}_N\cdot\mathbf{n})\; d\Gamma = \int_{\Gamma_f} [-\alpha\nabla\mathbf{u}_N : \nabla\mathbf{v}_N + \mathbf{f}\mathbf{v}_N]\mathbf{V}\cdot\mathbf{n}\; d\Gamma. \tag{65}$$

Utilizing (65) in (61), we find

$$\begin{aligned} dJ_2(\Omega,\mathbf{V}) &= \int_{\Gamma_f}\Big[\mathbf{f}\mathbf{v}_N - \alpha\nabla\mathbf{u}_N : \nabla\mathbf{v}_N + \mathcal{V}(\mathbf{n}\frac{\partial \mathbf{u}_N}{\partial \mathbf{n}} + \kappa\frac{1}{2}\mathcal{V})\Big]\mathbf{V}\cdot\mathbf{n}\; d\Gamma \\ &\quad - \int_{\Gamma_f} \mathcal{V}\mathbf{u}_N\nabla_{\Gamma_f}(\mathbf{V}\cdot\mathbf{n})\; d\Gamma. \end{aligned} \tag{66}$$

Applying the tangential Greens formula on the second integral in (66), we obtain

$$\int_{\Gamma_f} \mathcal{V}\mathbf{u}_N \nabla_{\Gamma_f}(\mathbf{V}\cdot\mathbf{n})\, d\Gamma = -\int_{\Gamma_f} \mathbf{V}\cdot\mathbf{n}\, \mathrm{div}_{\Gamma_f}(\mathcal{V}\mathbf{u}_N)\, d\Gamma + \int_{\Gamma_f} \kappa\mathcal{V}^2(\mathbf{v}_N)\, d\Gamma. \tag{67}$$

Utilizing the result in (67) in (66), we find

$$dJ_2(\Omega,\mathbf{V}) = \int_{\Gamma_f} [\mathbf{f}\mathbf{v}_N - \alpha\nabla\mathbf{u}_N : \nabla\mathbf{v}_N + \mathrm{div}_{\Gamma_f}(\mathcal{V}\mathbf{u}_N) + \mathcal{V}(\mathbf{n}\frac{\partial\mathbf{u}_N}{\partial\mathbf{n}} - \kappa\frac{1}{2}\mathcal{V})]\mathbf{V}\cdot\mathbf{n}\, d\Gamma, \tag{68}$$

as desired. □

4.2.3. *Shape derivative of J_3.* In order to obtain the shape derivative of the cost functional under consideration, more regularity of the state $(\mathbf{u}_D, p_D)$ is needed. Moreover, we need the following preliminary results to obtain this expression.

Proposition 4.5. *Let $\boldsymbol{f}\in\boldsymbol{H}^1(\Omega)$. Then for any $(\boldsymbol{u}_D, p_D)\in X\cap(\boldsymbol{H}^3(\Omega)\times H^2(\Omega))$, $J_3(\Omega)$ is differentiable in the directions $(\delta\boldsymbol{u}_D, \delta p_D)\in X\cap(\boldsymbol{H}^3(\Omega)\times H^2(\Omega))$ and the directional derivatives $J_3'(\Omega)\delta\boldsymbol{u}_D$, $J_3'(\Omega)\delta p_D$ are given by*

$$J_3'(\Omega)\delta\boldsymbol{u}_D = \int_{\Gamma_f}(-p_D\boldsymbol{n} + \alpha\frac{\partial\boldsymbol{u}_D}{\partial\boldsymbol{n}})\alpha\frac{\partial\delta\boldsymbol{u}_D}{\partial\boldsymbol{n}}\, d\Gamma, \tag{69}$$

$$J_3'(\Omega)\delta p_D = -\int_{\Gamma_f}(-p_D\boldsymbol{n} + \alpha\frac{\partial\boldsymbol{u}_D}{\partial\boldsymbol{n}})\delta p_D\boldsymbol{n}\, d\Gamma. \tag{70}$$

Proof. The proof follows from the definition of a directional derivative of a functional. □

Let $r := p_D - \alpha\frac{\partial\mathbf{u}_D}{\partial\mathbf{n}}\cdot\mathbf{n}$. Then, since $(\mathbf{u}_D, p_D)\in X\cap(\mathbf{H}^3(\Omega)\times H^2(\Omega))$, we have that $r\in\mathbf{H}^{3/2}(\Gamma_f)$. As a consequence of Proposition 4.5 and Theorem 4.3, there exists a unique $(\mathbf{v}_D, q_D)\in W_r(\Omega)\times L^2_0(\Omega)\cap(\mathbf{H}^2(\Omega)\times H^1(\Omega))$ such that

$$\alpha(\nabla\mathbf{v}_D, \nabla\boldsymbol{\psi})_\Omega - (q_D, \mathrm{div}\ \boldsymbol{\psi})_\Omega - (\mathrm{div}\ \mathbf{v}_D, \xi)_\Omega = 0, \text{ for all } (\boldsymbol{\psi}, \xi)\in X, \tag{71}$$

hold. Upon integration by parts, this amounts to

$$\begin{aligned} -\alpha\Delta\mathbf{v}_D + \nabla q_D &= 0, \quad \text{in} \quad \Omega,\\ \mathrm{div}\ \mathbf{v}_D &= 0, \quad \text{in} \quad \Omega,\\ \mathbf{v}_D &= 0, \quad \text{on} \quad \Gamma_D,\\ \mathbf{v}_D\cdot\mathbf{n} &= p_D - \alpha\frac{\partial\mathbf{u}_D}{\partial\mathbf{n}}\cdot\mathbf{n} \quad \text{on} \quad \Gamma_f,\\ \alpha\frac{\partial\mathbf{v}_D}{\partial\mathbf{n}}\cdot\boldsymbol{\tau} &= 0, \quad \text{on} \quad \Gamma_f. \end{aligned} \tag{72}$$

Proposition 4.6. *For $\boldsymbol{V}\in\mathcal{T}_{ad}$, the shape functional J_3 is shape differentiable with*

$$dJ_3(\Omega,\boldsymbol{V}) = \int_{\Gamma_f}[\mathcal{B} + div_\Gamma(\mathcal{R}(-p_D I + \alpha\nabla\boldsymbol{u}_D)) - \kappa\frac{\mathcal{R}^2}{2}]\boldsymbol{V}\cdot\boldsymbol{n}\, d\Gamma,$$

where $\mathcal{B} := \left(\boldsymbol{u}_D\nabla_\Gamma(\mathcal{S}_n) + (\boldsymbol{f} + \nabla_\Gamma(\sigma_{nn}) - \kappa\sigma_{nn}\boldsymbol{n})\boldsymbol{v}_D - \alpha\nabla\boldsymbol{u}_D\cdot\nabla\boldsymbol{v}_D + \mathcal{R}\frac{\partial\mathcal{R}}{\partial\boldsymbol{n}}\right)$, $\mathcal{R} := -p_D\boldsymbol{n} + \alpha\frac{\partial\boldsymbol{u}_D}{\partial\boldsymbol{n}}$, $\mathcal{S} := -q_D\boldsymbol{n} + \alpha\frac{\partial v_D}{\partial\boldsymbol{n}}$, $\mathcal{S}_n := \mathcal{S}\cdot\boldsymbol{n}$, $\mathcal{S}_{\boldsymbol{\tau}} := \mathcal{S}\cdot\boldsymbol{\tau}$, $\mathcal{R}_n := \mathcal{R}\cdot\boldsymbol{n}$, $\mathcal{R}_{\boldsymbol{\tau}} := \mathcal{R}\cdot\boldsymbol{\tau}$, *and all expressions are evaluated on* Γ_f *, with the adjoint state* $(\boldsymbol{v}_D, q_D)$ *satisfying (72).*

Proof. Since $J_3(\Omega)$ is differentiable with respect to $(\mathbf{u}_D, p_D)$, by Lemma 4.2 we obtain the Eulerian derivative of $J_3(\Omega)$ with respect to Ω:

$$dJ_3(\Omega,\mathbf{V}) = \int_\Gamma \mathcal{R}[\mathcal{R}' - (-p_D I + \alpha\nabla\mathbf{u}_D)\nabla_\Gamma(\mathbf{V}\cdot\mathbf{n}) + (\frac{\partial\mathcal{R}}{\partial\mathbf{n}} + \frac{\kappa}{2}\mathcal{R})\mathbf{V}\cdot\mathbf{n}\ ]\ d\Gamma, \tag{73}$$

where

$$\mathcal{R}' := (-p_D'\mathbf{n} + \alpha\frac{\partial\mathbf{u}_D'}{\partial\mathbf{n}}).$$

Multiplying the adjoint system (72) with $\mathbf{u}_D'$, we obtain

$$(\nabla\mathbf{v}_D, \nabla\mathbf{u}_D')_\Omega - (q_D, \operatorname{div}\mathbf{u}_D')_\Omega = (\mathcal{S}, \mathbf{u}_D')_{\Gamma_f}. \tag{74}$$

On the other hand, multiplying the sensitivity equation in (37) with the adjoint vector field $\mathbf{v}_D$, we find

$$(\nabla\mathbf{v}_D, \nabla\mathbf{u}_D')_\Omega - (p_D', \operatorname{div}\mathbf{v}_D)_\Omega = (\mathcal{R}', \mathbf{v}_D)_{\Gamma_f}. \tag{75}$$

From (74) and (75), we obtain

$$(\mathcal{S}, \mathbf{u}_D')_{\Gamma_f} = (\mathcal{R}', \mathbf{v}_D)_{\Gamma_f}. \tag{76}$$

Splitting the left and right hand sides of (76) in component wise form, we arrive at

$$(\mathcal{S}_n, \mathbf{u}_D'\cdot\mathbf{n})_{\Gamma_f} + (\mathcal{S}_{\boldsymbol{\tau}}, \mathbf{u}_D'\cdot\boldsymbol{\tau})_{\Gamma_f} = \int_{\Gamma_f}(\mathcal{R}_n')\mathbf{v}_D\cdot\mathbf{n} + (\mathcal{R}_{\boldsymbol{\tau}}')\ \mathbf{v}_D\cdot\boldsymbol{\tau}\ d\Gamma, \tag{77}$$

where $\mathcal{R}_n' := \mathcal{R}'\cdot\mathbf{n}$, $\mathcal{R}_{\boldsymbol{\tau}}' := \mathcal{R}'\cdot\boldsymbol{\tau}$. Observe that the second term on the left hand side of (77) vanishes since $\mathcal{S}_{\boldsymbol{\tau}} = \alpha\frac{\partial\mathbf{v}_D}{\partial\mathbf{n}}\cdot\boldsymbol{\tau} = 0$ (c.f., system (72)). Hence, since $\mathbf{v}_D\cdot\mathbf{n} = -\mathcal{R}_n$, we have

$$\int_{\Gamma_f}\mathcal{R}_n'\mathcal{R}_n\ d\Gamma = -\int_{\Gamma_f}\mathcal{S}_n\ \mathbf{u}_D'\cdot\mathbf{n}\ d\Gamma + \int_{\Gamma_f}\mathcal{R}_{\boldsymbol{\tau}}'\ \mathbf{v}_D\cdot\boldsymbol{\tau}\ d\Gamma. \tag{78}$$

Substituting the boundary conditions satisfied by $\mathbf{u}_D'\cdot\mathbf{n}$ on Γ_f into the first integral in (78), one obtains

$$-\int_{\Gamma_f}\mathcal{S}_n\ \mathbf{u}_D'\cdot\mathbf{n}\ d\Gamma = -\int_{\Gamma_f}\mathcal{S}_n\ \operatorname{div}_\Gamma(\mathbf{u}_D(\mathbf{V}\cdot\mathbf{n}))\ d\Gamma. \tag{79}$$

The integral on the right hand side of (79) can be further simplified by utilizing the tangential Green's formula, such that

$$-\int_{\Gamma_f}\mathcal{S}_n\ \operatorname{div}_\Gamma(\mathbf{u}_D(\mathbf{V}\cdot\mathbf{n}))\ d\Gamma = \int_{\Gamma_f}\mathbf{u}_D\nabla_\Gamma(\mathcal{S}_n)\ d\Gamma. \tag{80}$$

Let us now turn the second integral on the right hand side of (78) and observe that $\mathcal{R}' = \sigma(\mathbf{u}_D', p_D')\cdot\mathbf{n}$. Hence, utilizing Proposition 4.1 and Remark 4.2 with $\boldsymbol{\psi} = \mathbf{v}_D$, we can express the second integral in (78) as

$$\int_{\Gamma_f} \mathcal{R}_{\boldsymbol{\tau}}' \mathbf{v}_D \cdot \boldsymbol{\tau}\, d\Gamma = \int_{\Gamma_f} \Big\{ -\sigma_{nn}\mathrm{div}_\Gamma(\mathbf{v}_D(\mathbf{V}\cdot\mathbf{n})) - [\alpha\nabla\mathbf{u}_D\cdot\nabla\mathbf{v}_D - \mathbf{f}\cdot\mathbf{v}_D]\mathbf{V}\cdot\mathbf{n}\Big\}\, d\Gamma, \tag{81}$$

Utilizing the tangential Green's formula, we can express the first addend on the right hand side of (81) as

$$\int_{\Gamma_f} -\sigma_{nn}\mathrm{div}_\Gamma(\mathbf{v}_D(\mathbf{V}\cdot\mathbf{n}))\, d\Gamma = \int_{\Gamma_f} \Big\{\mathbf{v}_D\cdot\nabla_\Gamma(\sigma_{nn}) - \kappa\sigma_{nn}(\mathbf{v}_D\cdot\mathbf{n})\Big\}\mathbf{V}\cdot\mathbf{n}$$

Hence

$$\int_{\Gamma_f} \mathcal{R}_n\mathcal{R}_n'\, d\Gamma = \int_{\Gamma_f} \Big\{\mathbf{u}_D\nabla_\Gamma(\mathcal{S}_n) + (\mathbf{f} + \nabla_\Gamma(\sigma_{nn}) - \kappa\sigma_{nn}\mathbf{n})\mathbf{v}_D - \alpha\nabla\mathbf{u}_D\cdot\nabla\mathbf{v}_D\Big\}\mathbf{V}\cdot\mathbf{n}\, d\Gamma.$$

Observe that since $\mathcal{R}\cdot\boldsymbol{\tau} = 0$, we have that $\int_{\Gamma_f}\mathcal{R}\mathcal{R}'\, d\Gamma = \int_{\Gamma_f}\mathcal{R}_n\mathcal{R}_n'\, d\Gamma$. Thus

$$\begin{aligned} dJ_3(\Omega,\mathbf{V}) &= \int_{\Gamma_f} \Big\{\mathbf{u}_D\nabla_\Gamma(\mathcal{S}_n) + (\mathbf{f} + \nabla_\Gamma(\sigma_{nn}) - \kappa\sigma_{nn}\mathbf{n})\mathbf{v}_D - \alpha\nabla\mathbf{u}_D\cdot\nabla\mathbf{v}_D\Big\}\mathbf{V}\cdot\mathbf{n}\, d\Gamma \\ &\quad + \int_{\Gamma_f} \mathcal{R}[-(-p_D I + \alpha\nabla\mathbf{u}_D)\nabla_\Gamma(\mathbf{V}\cdot\mathbf{n}) + (\frac{\partial\mathcal{R}}{\partial\mathbf{n}} + \frac{\kappa}{2}\mathcal{R})\mathbf{V}\cdot\mathbf{n}\ ]\, d\Gamma, \\ &= \int_{\Gamma_f}\Big\{\mathcal{B} + \frac{\kappa}{2}\mathcal{R}^2\Big\}\mathbf{V}\cdot\mathbf{n}\, d\Gamma - \int_{\Gamma_f}\mathcal{R}(-p_D I + \alpha\nabla\mathbf{u}_D)\nabla_\Gamma(\mathbf{V}\cdot\mathbf{n})\, d\Gamma. \end{aligned} \tag{82}$$

Applying the tangential Green's formula on the second integral in (82) gives

$$\int_{\Gamma_f}\mathcal{R}(-p_D I + \alpha\nabla\mathbf{u}_D)\nabla_\Gamma(\mathbf{V}\cdot\mathbf{n})\, d\Gamma = \int_{\Gamma_f}[-\mathrm{div}_\Gamma(\mathcal{R}(-p_D I + \alpha\nabla\mathbf{u}_D)) + \kappa\mathcal{R}^2]\mathbf{V}\cdot\mathbf{n}\, d\Gamma. \tag{83}$$

Combining (82) and (83) gives the desired results. □

Remark 4.3. *In this section, we have shown that the shape derivatives of cost functionals J_i, $i = 1,2,3$ can be written in the form*

$$dJ_i(\Omega,\boldsymbol{V}) = \int_{\Gamma_f} G_i\boldsymbol{V}\cdot\boldsymbol{n}\, d\Gamma, \quad i = 1,2,3 \tag{84}$$

where

$$G_1 := \Big(\frac{\alpha}{2}|\nabla\boldsymbol{w}|^2 + \alpha\nabla\boldsymbol{u}_N\nabla\boldsymbol{w} - \boldsymbol{f}\boldsymbol{w} - \boldsymbol{u}_D\nabla_\Gamma(-q + \alpha\frac{\partial\boldsymbol{w}}{\partial\boldsymbol{n}}\boldsymbol{n})\Big), \tag{85}$$

$$G_2 := [\boldsymbol{f}\boldsymbol{v}_N - \alpha\nabla\boldsymbol{u}_N : \nabla\boldsymbol{v}_N + div_{\Gamma_f}(\mathcal{V}\boldsymbol{u}_N) + \mathcal{V}(\boldsymbol{n}\frac{\partial\boldsymbol{u}_N}{\partial\boldsymbol{n}} - \kappa\frac{1}{2}\mathcal{V})],\ \textit{and} \tag{86}$$

$$G_3 := [\mathcal{B} + div_\Gamma(\mathcal{R}(-p_D I + \alpha\nabla\boldsymbol{u}_D)) - \kappa\frac{\mathcal{R}^2}{2}], \tag{87}$$

are well defined functions of Γ*. Note that the computation of* G_2 *and* G_3 *involve not only the computation of the respective states and adjoint equations, but also the evaluation of the mean curvature* κ *of* Γ_f*. This may be evaluated as*

$$\kappa := div_\Gamma(\mathbf{n}_\varepsilon), \tag{88}$$

where $\mathbf{n}_\varepsilon \in H^1(\Gamma)$ *is the smoothed normal vector field on the free boundary* Γ_f *satisfying*

$$\int_{\Gamma_f} \varepsilon \nabla_\Gamma \boldsymbol{n}_\varepsilon \nabla_\Gamma \varphi + \boldsymbol{n}_\varepsilon \varphi \; d\Gamma = \int_{\Gamma_f} \boldsymbol{n}\varphi \; d\Gamma, \textit{ for all } \varphi \in H^1(\Gamma), \tag{89}$$

and ε *is some fixed small parameter.*

5. Numerical algorithm and examples

The numerical solution of (7) consists in adopting an iterative procedure that decreases the value of the cost functional $J_i,\ i = 1,2,3$ at each iteration. Let us denote by Γ_f^k, the free boundary at the kth iteration. Then at the $(k+1)$th iterative step, the free boundary Γ_f^{k+1} becomes

$$\Gamma_f^{k+1} = \left\{ x + t\mathbf{V}(x);\ x \in \Gamma_f^k \right\}, \tag{90}$$

where $t \geq 0$ is a sufficiently small step size parameter and $\mathbf{V}$ is chosen such that it provides a decent direction for the cost J_i. If such a $\mathbf{V}$ exists, then it should satisfy the equation

$$\langle \mathbf{V}, \varphi \rangle_{\mathcal{X}} = -\langle G_i \mathbf{n}, \varphi \rangle_{L^2(\Gamma_f)}, \tag{91}$$

for all φ chosen from some appropriately chosen functional space $\mathcal{X}$. If we choose $\mathcal{X} := L^2(\Gamma_f)$, then $\mathbf{V}|_{\Gamma_f} = -G_i\mathbf{n}$ and for this choice, $dJ_i(\Omega, \mathbf{V}) < 0$. However, this choice of $\mathbf{V}$ may lead to subsequent loss of regularity of Γ_f hence creating oscillations of Γ_f [33, 21]. In this work, we chose $\mathcal{X} := \mathbf{H}^1(\Omega)$ and utilize (91) to compute $\mathbf{V}$. The resulting vector field $\mathbf{V}$ (also known in some literature as Sobolev gradient [29]) provides an extension of $G_i\mathbf{n}$ over the entire domain which may as well be shown to have a regularizing effect on the boundary Γ_f (c.f., [33, 21, 14]).

To numerically implement (90), one has to find a suitable parametrization of the admissible shapes using a finite number of parameters. Here, we utilize the positioning of boundary nodes of a partition into finite elements as design parameters.

5.1. The boundary variation algorithm.

Let Γ_f^0, Γ_f^F denote the free boundaries corresponding to the initial and final domains Ω_0 and Ω_F, respectively. Then the steps required for the computation of the kth domain using cost J_1 are summarized in Algorithm 1.

Remark 5.1. *The* $\mathbf{H}^1(\Omega)$ *norm of* $\boldsymbol{V}$ *together with the maximum value of* $\boldsymbol{V}$ *on* Γ_f *are used as the stopping criteria for the optimization Algorithm 1, i.e., the algorithm is stopped as soon as* $\max(\|\boldsymbol{V}\|_{\mathbf{H}^1}, \|\boldsymbol{V}\|_{C(\Gamma_f)})$ *is sufficiently small. During each optimization step, the step size* t_j *is chosen on the basis of the Armijo-type line search and such that there are no reversed triangles within the mesh after the update.*

Algorithm 1 The boundary variation algorithm (Problem 1)

- Choose initial shape Ω_0;
- Compute the states $(\mathbf{u}_D, p_D)$ and $(\mathbf{u}_N, p_N)$ using the Taylor-Hood finite element, then evaluate the descent direction $\mathbf{V}_k$ by using (91), which amounts to solving the following system

$$-\Delta \mathbf{V} + \mathbf{V} = 0 \text{ in } \Omega, \tag{92}$$

$$\frac{\partial \mathbf{V}}{\partial \mathbf{n}} = -G_1 \mathbf{n} \text{ on } \Gamma_f, \tag{93}$$

$$\mathbf{V} = 0 \text{ on } \Gamma_D, \tag{94}$$

with $\Omega = \Omega_k$;
- Set $\Omega_{k+1} = (Id + t_k \mathbf{V}_k)\Omega_k$ where t_k is a positive scalar.

Remark 5.2. *In the case of costs J_2 and J_3, the second step in Algorithm 1 is modified. The states $(\boldsymbol{u}_D, p_D)$, $(\boldsymbol{u}_N, p_N)$ and their respective adjoint variables are computed using the Taylor-Hood finite element. Then the mean curvature κ of Γ_f is determined using* (88) *and the descent direction $\mathbf{V}_k$ at the k^{th} iterative step is evaluated by using* (92)-(94).

5.2. **Numerical example 1.** In this example, we consider a gravity like force $\mathbf{f}$=$(-10x,\ -10y)$ which keeps the fluid on top of the circular domain (radius 0.4) (c.f., Figure 1 (a)). The motion of the fluid is triggered by an initial velocity. We expect that as the fluid comes to rest, a free surface position, which is concentric with the circular domain, is attained [6].

Homogenous Dirichlet boundary conditions are imposed on the fixed boundary Γ_D and we set the value of α to 0.01. The location of the initial fluid free boundary location Γ_f^0 is set as

$$\Gamma_f^0 := \left\{ (x,y) \in \mathbb{R}^2 \ : \ \frac{x^2}{1} + \frac{y^2}{1.2^2} = 1 \right\}. \tag{95}$$

The resulting computational domain in Figure 1 (a) is discretized by triangular elements generated by the bi-dimensional anisotropic mesh generator [13]. The Navier-Stokes equations (9) and (10) are then discretized using the Galerkin finite-element method. We use Taylor-Hood elements for the approximation velocity and pressure. This results in a set of linear algebraic equations that may be represented in matrix form as

$$\mathbf{K}\bar{\mathbf{u}} = \mathbf{F}, \tag{96}$$

where $\mathbf{K}$ is the global system matrix, $\bar{\mathbf{u}}$ is the global vector of unknowns (velocities and pressures), and $\mathbf{F}$ is a vector that includes the effects of body forces and boundary conditions. This linear system is solved by a multi-frontal Gauss LU factorization implemented in the package UMFPACK [8]. The flow field patterns in Figures 2(a) and 2(b) are obtained. In Figure 2(b), the flow field lines for $\mathbf{u}_N$ point out of Γ_f and therefore, do not satisfy $\mathbf{u}_N \cdot \mathbf{n} = 0$ on Γ_f. Moreover, the magnitude of $\mathbf{u}_N$ is seen to be dominating that of the flow field $\mathbf{u}_D$ (Figure 2(a)). Hence, the vector field $\mathbf{w} \approx -\mathbf{u}_N$ (Figure 2(c)) and clearly, these two flow fields do not match, see Figure 2(c).

5.2.1. *Optimization with J_1.* To narrow the gap between the two flow fields $\mathbf{u}_D$ and $\mathbf{u}_N$, we run Algorithm 1 until $\max(\|\mathbf{V}\|_{\mathbf{H}^1}, \|\mathbf{V}\|_{C(\Gamma_f)}) < 10^{-5}$. This stopping criterion is met after 43 iterations

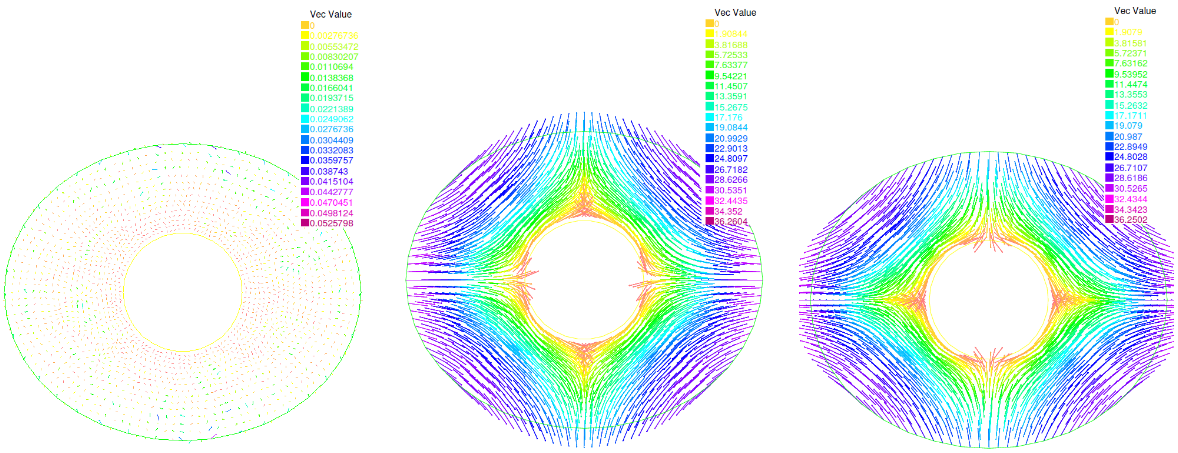

(a) Initial flow $\mathbf{u}_D$ (b) Initial flow $\mathbf{u}_N$ (c) Initial flow $\mathbf{w} := \mathbf{u}_D - \mathbf{u}_N$

Figure 2. Flow on initial domain

with the final value of the cost of magnitude 2.23×10^{-6}. The corresponding geometry and flow fields solving the free surface problem are depicted in Figures 3(a-b).

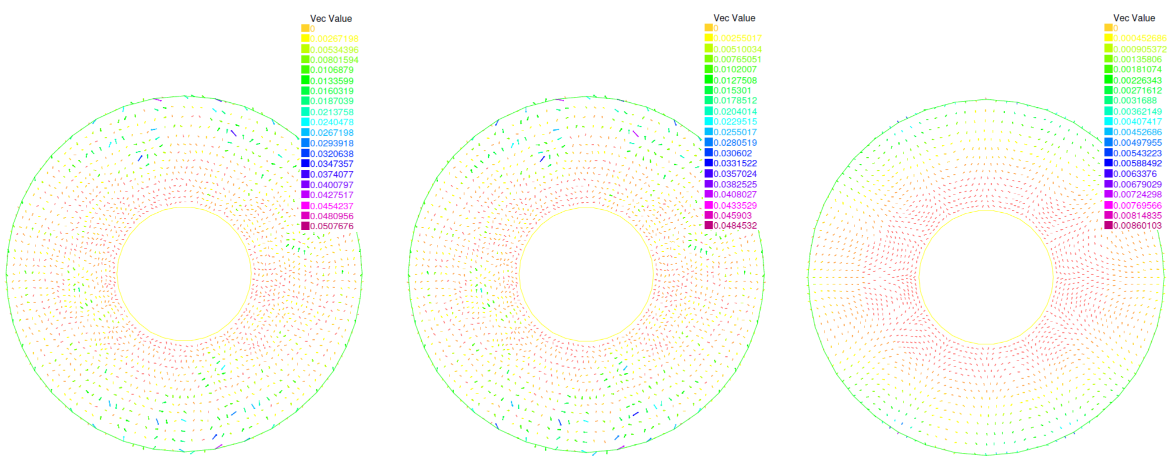

(a) Final flow $\mathbf{u}_D$ (b) Final flow $\mathbf{u}_N$ (c) Final flow $\mathbf{w} := \mathbf{u}_D - \mathbf{u}_N$

Figure 3. Flow on final domain

In Figures 3 (a-b), we observe that both vector fields $\mathbf{u}_D$ and $\mathbf{u}_N$ vanish at the solution of the free surface problem (7). Moreover, as expected, the free surface position is concentric with the circular domain and the final velocity field $\mathbf{u} = 0$.

A plot of the three costs vs iteration results in graphs depicted in Figures 4(a). The graphs in Figures 4(a) are obtained by evaluating $J_i, 1 = 1, 2, 3$, along the iterates of minimizing J_1.

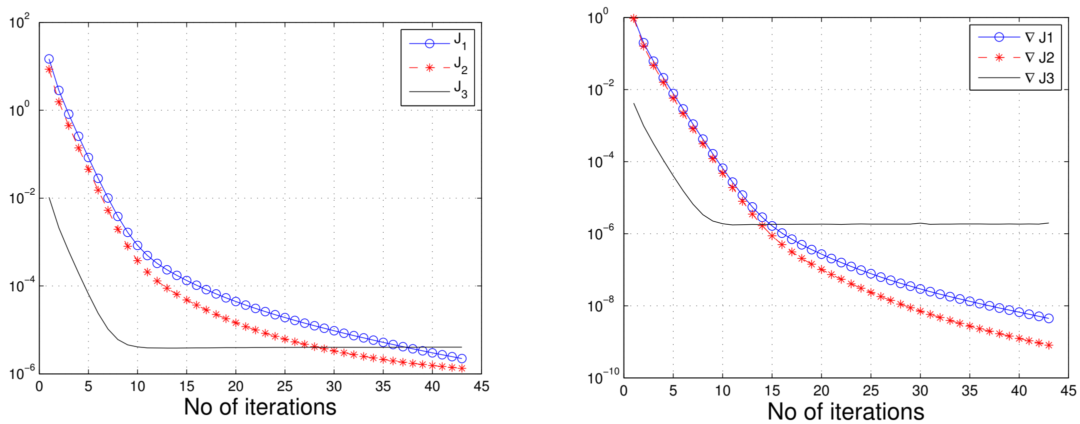

(a) Histories of shape functionals

(b) History of gradient norm

FIGURE 4. Histories of shape functionals and gradients

From Figure 4 (a), we observe that as the iteration count increases, all the cost functionals decrease as expected. We also observe that after 11 iterations, cost functional J_2 goes down faster than J_1 while cost J_3 slows down. In order to investigate the convergence of the three functionals, the histories of the gradient norms of the three functionals are plotted in Figure 4 (b). The values of the gradient norm for cost functional J_2 are scaled by a factor 10^{-3}. From this figure, we observe that both J_1 and J_2 converge with the same rate with J_2 decreasing faster than J_1 after 11 iterations. The convergence of cost J_3 slows down after 9 iterations which possibly indicates that it is algebraically ill-posed. This implies that it may be insensitive with respect to geometric perturbation in this example. We shall investigate this aspect in the following sub-subsection.

5.2.2. *Optimization with J_2 and J_3.* In order to validate the findings of the previous sub-subsection as well as to check whether the computed shape gradients for J_2 and J_3 in (86) and (87), respectively, actually produce descent directions for their respective costs, Algorithm 1 is modified according to Remark 5.2. We run Algorithm 1 until $\max(\|\mathbf{V}\|_{\mathbf{H}^1}, \|\mathbf{V}\|_{C(\Gamma_f)})$ is less than 10^{-4}, 10^{-6} for cost functionals J_2 and J_3, respectively. These stopping criteria are met after 30 and 65 iterations, for cost functionals J_2 and J_3, respectively. The final value of J_2 is found to be 2.25×10^{-5} while that of J_3 is 4.06×10^{-6}. The final boundaries Γ_f^{KV}, Γ_f^{NV} and Γ_f^{NS} corresponding to the minimization of cost functionals J_1, J_2 and J_3, respectively, are depicted in Figure 5. For given points $A(x_i^{NV}, y_i^{NV})$ and $B(x_i^{NS}, y_i^{NS})$, on Γ_f^{NV} and Γ_f^{NS}, respectively, with $i = 1, \ldots, d$ where d is the number of discretization points on the boundary Γ_f, the distance $d(\Gamma_f^{NS}, \Gamma_f^{NV})$ between Γ_f^{NS} and Γ_f^{NV} is evaluated via by the formula

$$d(\Gamma_f^{NS}, \Gamma_f^{NV}) = \max_i \sqrt{(x_i^{NV} - x_i^{NS})^2 + (y_i^{NV} - y_i^{NS})^2}.$$

Analogously, the distances $d(\Gamma_f^{KV}, \Gamma_f^{NV})$ and $d(\Gamma_f^{KV}, \Gamma_f^{NS})$ are computed. The maximum of the distances $d(\Gamma_f^{KV}, \Gamma_f^{NV})$, $d(\Gamma_f^{KV}, \Gamma_f^{NS})$, $d(\Gamma_f^{NS}, \Gamma_f^{NV})$, is computed and is found to be of order 10^{-3}. This

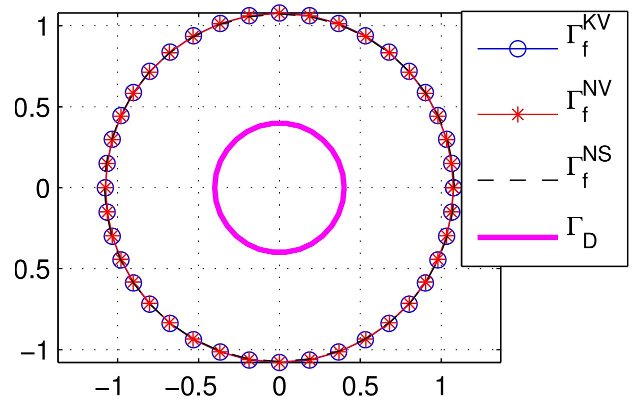

FIGURE 5. Final outer boundaries

implies that the final boundaries Γ_f corresponding to the minimization of each of the three cost functionals coincide (see Figure 5).

The high number of iterations required for the minimization of J_3 suggests that it is insensitive with respect to geometric perturbations in this example. Since the number of iterations for J_2 is less than that for J_1 and J_3, we can conclude that J_2 is more sensitive than J_1 and J_3, which agrees with the findings from the previous sub-subsection. However, the higher convergence of J_2 is achieved at the expense of the higher computation cost involved in evaluating its shape gradient (See Remark 4.3).

5.3. **Numerical example 2.** In this example, we determine the location of the free surface at the upper boundary, for a two dimensional cavity with fixed vertical side walls and a driven floor (Figure 1 (b)). The flow in the cavity is subjected to a body force $\mathbf{f} = (-1.2, 0)$ and the parameter α is set to 0.0125.

The dimensions of the cavity are chosen as $\Omega := (0,1) \times (0,1)$. The floor $\Gamma_b := \{(x,y) \in \Omega : \ y = 0\}$ of the cavity is driven by the velocity field $\mathbf{u} = (4x(x-1), 0)$. On the fixed vertical walls $\Gamma_w := \{(x,y) \in \Omega : \ (x = 0) \cup (x = 1)\}$, we impose the slip boundary condition $\mathbf{u} \cdot \mathbf{n} = 0$, $\alpha \frac{\partial \mathbf{u}}{\partial \mathbf{n}} \cdot \boldsymbol{\tau} = 0$, and on $\Gamma_f := \{(x,y) \in \Omega : \ y = 1\}$, boundary conditions analogous to the ones in (5) are imposed. The resulting computational domain is discretized by triangular elements generated by the bi-dimensional anisotropic mesh generator. The discretization of the continuous flow equations and the numerical solution of the resultant linear systems proceeds as explained in the previous section. The flow field patterns in Figures 6(a) and 6(b) are obtained.

In Figure 6(a), the velocity field lines are tangential to Γ_f. Evidently, the flow field satisfy $\mathbf{u}_D \cdot \mathbf{n} = 0$ on Γ_f, although the normal component of the normal stress is non-zero at this boundary. On the other hand, in Figure 6(b), the flow field lines for $\mathbf{u}_N$ point out of Γ_f and therefore, do not satisfy $\mathbf{u}_N \cdot \mathbf{n} = 0$ on Γ_f. Indeed, initially these two flow fields do not match, see Figure 6(c). To narrow the gap between $\mathbf{u}_D$ and $\mathbf{u}_N$, we run Algorithm 1 until $\max(\|\mathbf{V}\|_{\mathbf{H}^1}, \|\mathbf{V}\|_{C(\Gamma_f)}) < 10^{-3}$. This stopping criterion is met after 18 iterations with the final value of the cost of magnitude

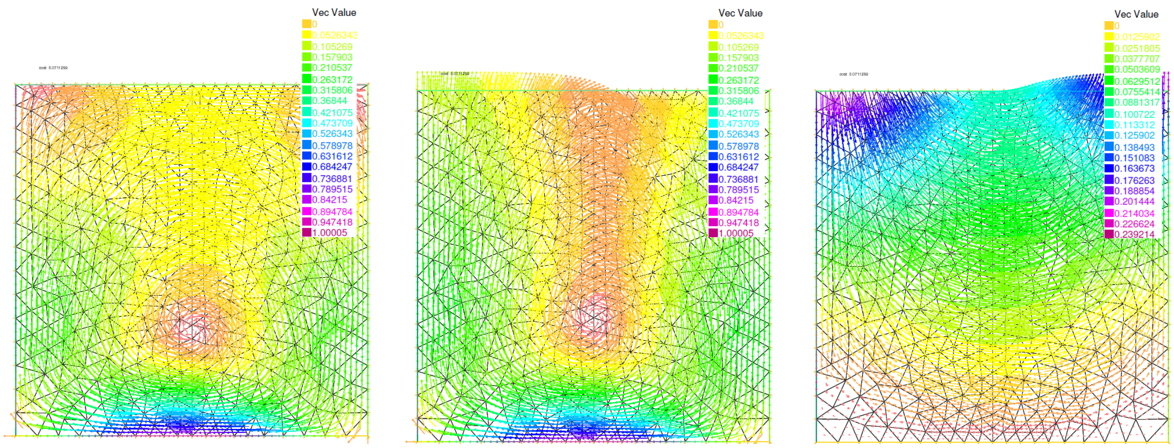

(a) Initial flow $\mathbf{u}_D$ (b) Initial flow $\mathbf{u}_N$ (c) Initial flow $\mathbf{w}$

FIGURE 6. Flow on initial domain

3.37×10^{-5}. The corresponding geometry and flow fields solving the free surface problem are depicted in Figures 6(a) and (b). We observe that on Ω_F, the flow field lines for $\mathbf{u}_N$ are tangential

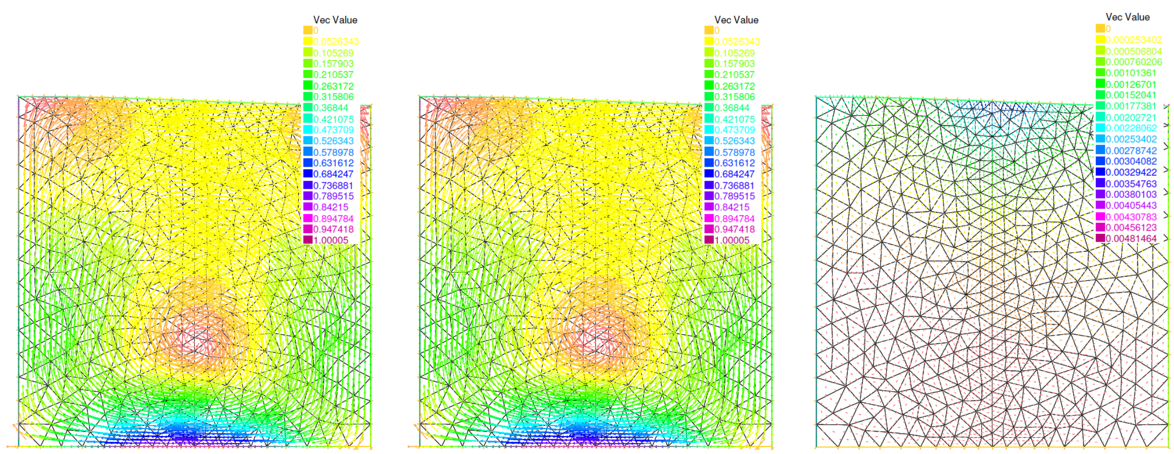

(a) Final flow $\mathbf{u}_D$ (b) Final flow $\mathbf{u}_N$ (c) Final flow $\mathbf{w}$

FIGURE 7. Flow on final domain

to Γ_f and hence satisfy $\mathbf{u}_N \cdot \mathbf{n} = 0$ on Γ_f. Furthermore, the maximum value of the vector field $\mathbf{w}$ is found to be of order 10^{-3} implying the both fields for $\mathbf{u}_D$ and $\mathbf{u}_N$ match each other of the final shape. A plot of the three costs vs iteration results in graphs depicted in Figures 8 (a). The graphs in Figures 8 (a) are obtained by evaluating $J_i, 1 = 1, 2, 3$, along the iterates of minimizing J_1. The values of cost functional J_2 are scaled by a factor of 2.83. From these figures, we observe that as the iteration count increases, both J_1 and J_2 decrease while J_3 oscillates possibly due to lack of regularity. We also observe that after 11 iterations, cost functional J_2 decreases faster than

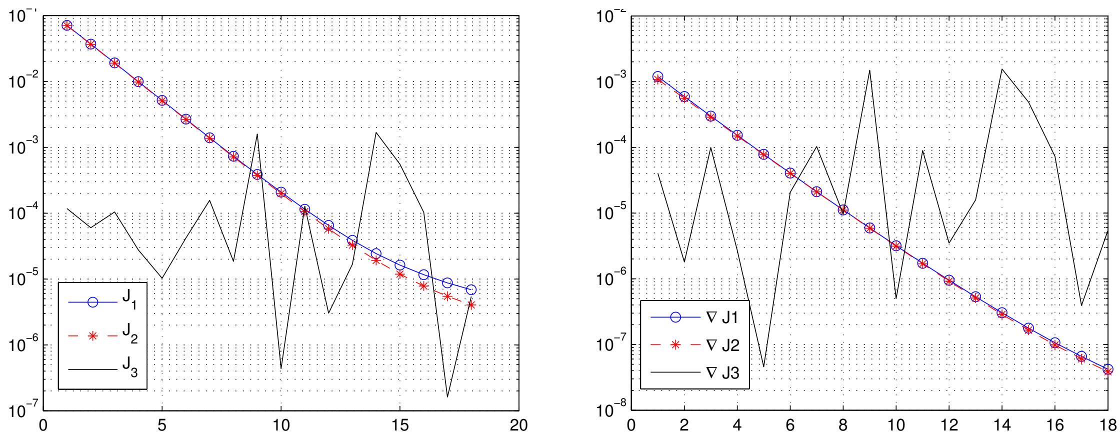

(a) History of the functionals (b) History of the gradient norms

Figure 8. Histories of shape functionals and the gradients

J_1. In order to investigate the convergence of the three functionals, the histories of the gradient norms of the three functionals are plotted in Figure 8 (b). The values of the gradient norm for cost functional J_2 are scaled by a factor 10^{-3}. From this figure, we observe that both J_1 and J_2 converge with the same rate with J_2 decreasing faster than J_1 after 11 iterations. The gradient norm for J_3 is found to be of order 10^{-5}. This implies that it may be insensitive with respect to geometric perturbation in this example. This phenomenon is actually observed when the computations are performed with cost functional J_3.

Conclusions

We proposed different cost functionals to reformulate free surface problems into shape optimization problems. Shape gradients of the cost functionals were derived and a steepest descent algorithm was implemented. The numerical results show the convergence of the proposed algorithm to an approximate solution of the free surface problem. It is found that the normal stress cost functional is insensitive with respect to geometric perturbations while the normal velocity converge slightly faster than the energy gap functional at the expense of computing the mean curvature of the free surface, to evaluate its shape gradient. It remains to investigate analytically the algebraic well-posedness or ill-posedness of the proposed cost functionals as well as extending the proposed optimization approaches to flows where surface tension is incorporated into the free surface model.

References

[1] B. Alessandrini and G. Delhommeau. Simulation of three-dimensional unsteady viscous free surface flow around a ship model. *Int. J. Num. Meth. Fluids*, 19(4):321–342, 1994.

[2] M. Badra, F. Caubet, and M. Dambrine. Detecting an obstacle immersed in a fluid by shape optimization methods. *Math. Models Methods Appl. Sci*, 21(10):2069–2101, 2011.

[3] A. Ben Abda, F. Bouchon, G.H. Peichl, M. Sayeh, and R. Touzani. A Dirichlet-Neumann cost functional approach for the Bernoulli problem. *J. Engrg. Math*, pages 1–20, 2013.

[4] F. Caubet, M. Dambrine, D. Kateb, and C. Z. Timimoun. A Kohn-Vogelius formulation to detect an obstacle immersed in a fluid. *Inverse Probl. Imaging*, 7(1):123–157, 2013.
[5] G. Cerne, S. Petelin, and I. Tiselj. Numerical errors of the volume-of-fluid interface tracking algorithm. *Int. J. Num. Meth. Fluids*, 38:329–350, 2002.
[6] Comsol. Femlab 3 multiphysics modeling guide. http://www.femlab.com, 2004.
[7] C. Cuvelier and R. M. S. M. Schulkes. Some numerical methods for the computation of capillary free boundaries governed by the Navier-Stokes equations. *SIAM Rev*, 32(3):355–423, 1990.
[8] T. A. Davis and I. S. Duff. A combined unifrontal/multifrontal method for unsymmetric sparse matrices. *ACM Trans. Math. Softw*, 25(1):1–20, 1999.
[9] M. C. Delfour and J. P. Zolésio. *Shapes and geometries: analysis, differential calculus, and optimization*. Society for Industrial and Applied Mathematics, Philadelphia, PA, USA, 2001.
[10] R. Dziri and J. P. Zolésio. *An Energy Principle for a Free Boundary Problem for Navier-Stokes Equations*. In Partial differential equation methods in control and shape analysis, pages 133–151. Lecture Notes in Pure and Appl. Math., 188, Dekker, New York, 1997.
[11] K. Eppler and H. Harbrecht. On a Kohn-Vogelius like formulation of free boundary problems. *Comput. Optim. Appl*, 52:69–85, 2012.
[12] V. Girault and P. A. Raviart. *Finite Element Methods for Navier-Stokes*. Springer-Verlag, Berlin, 1986.
[13] F. Hecht and O. Pironneau. Freefem++ manual, laboratoire jacques louis lions,freefem++ is a free software available at:. http://www-rocq.inria.fr/Frederic.Hecht/freefem++.html, 2005.
[14] A. Henrot and Y. Privat. What is the optimal shape of a pipe? *Arch. Ration. Mech. Anal*, 196(1):281–302, 2009.
[15] C.W. Hirt and B.D. Nichols. Volume of fluids methods for the dynamics of free boundaries. *J. Comput. Phys*, 39:201–225, 1981.
[16] K. Ito, K. Kunisch, and G. Peichl. Variational approach to shape derivatives for a class of Bernoulli problems. *J. Math. Anal. Appl*, 314(1):126–149, 2006.
[17] K. Ito, K. Kunisch, and G. Peichl. Variational approach to shape derivatives. *ESAIM Control Optim. Calc. Var*, 14:517–539, 2008.
[18] K. T. Kärkkäinen and T. Tiihonen. Free surfaces: shape sensitivity analysis and numerical methods. *Int. J. Numer. Meth. Engrg*, 44(8):1079–1098, 1999.
[19] Kari T. Kärkkäinen and Timo Tiihonen. Free surfaces: shape sensitivity analysis and numerical methods. *Internat. J. Numer. Methods Engrg*, 44(8):1079–1098, 1999.
[20] H. Kasumba and K. Kunisch. On free surface pde constrained shape optimization problems. *Appl. Math. Comput*, 218(23):11429 – 11450, 2012.
[21] H. Kasumba and K. Kunisch. Vortex control in channel flows using translation invariant cost functionals. *Comput. Optim. Appl*, 52(3):691–717, 2012.
[22] M. Kawahara and B. Ramaswamy. Lagrangian finite element analysis applied to viscous free surface fluid flow. *Internat. J. Numer. Methods Engrg*, 953(7), 1987.
[23] R. Kohn and M. Vogelius. Determining conductivity by boundary measurements. *Comm. Pure Appl. Math*, 37:289–298, 1984.
[24] A. Laurain and Y. Privat. On a bernoulli problem with geometric constraints. *ESAIM Control Optim. Calc. Var*, 18(1):157–180, 2 2012.
[25] Alex G. Lee, Eric S. G. Shaqfeh, and Bamin Khomami. A study of viscoelastic free surface flows by the finite element method: Hele-shaw and slot coating flows. *J. Non-Newt. Fluid Mech*, 108(1-3):327 – 362, 2002.
[26] A. Liakos. Discretization of the Navier-Stokes equations with slip boundary condition. *Numer. Methods Partial Differential Equations*, 17(1):26–42, 2001.
[27] F. Losasso, R. Fedkiw, and S. Osher. Spatially adaptive techniques for level set methods and incompressible flow. *Comput. & Fluids*, 35(10):995 – 1010, 2006.
[28] H. Miyata. Finite-difference simulation of breaking waves. *J. Comput. Phys*, 65(1):179–214, July 1986.
[29] J. Neuberger. *Sobolev Gradients and Differential Equations*. Lecture Notes in Mathematics, Series Editors: Morel, Jean-Michel, Teissier, Bernard. Springer, Berlin, 2010.

[30] S. Osher and J. A. Sethian. Fronts propagating with curvature-dependent speed: algorithms based on Hamilton-Jacobi formulations. *J. Comput. Phys*, 79(1):12–49, 1988.
[31] G. Panaras, A. Theodorakakos, and G. Berggeles. Numerical investigation of the free surface in a continuous steel casting mold model. *Metall. Mater. Trans. B*,, 29:1117–1126, 1998. 10.1007/s11663-998-0081-3.
[32] R. C. Peterson, P. K. Jimack, and M. A. Kelmanson. The solution of two-dimensional free-surface problems using automatic mesh generation. *Internat. J. Numer. Methods Fluids*, 31(6):937–960, 1999.
[33] O. Pironneau and B. Mohammadi. *Applied Shape optimization in Fluids*. Oxford University Press Inc, Newyork, 2001.
[34] J. Sokolowski and J. P. Zolésio. *Introduction to Shape Optimization. Shape Sensitivity Analysis*. Springer-Verlag, 1992.
[35] E. H. van Brummelen, H. C. Raven, and B. Koren. Efficient numerical solution of steady free-surface Navier-Stokes flow. *J. Comput. Phys*, 174(1):120–137, November 2001.
[36] E. H. Van Brummelen and A. Segal. Numerical solution of steady free-surface flows by the adjoint optimal shape design method. *Internat. J. Numer. Methods Fluids*, 41(1):3–27, 2003.
[37] E. P. VanLohuizen, P. J. Slikkerveer, and S. B. G. O'Brien. An implicit surface tension algorithm for picard solvers of surface-tension-dominated free and moving boundary problems. *Internat. J. Numer. Methods Fluids*, 22(9):851–65, 1996.
[38] O. Volkov, B. Protas, W. Liao, and D. W. Glander. Adjoint-based optimization of thermo-fluid phenomena in welding processes. *J. Eng. Math*, 65(3):201–220, 2009.
[39] S. Wei, R. W. Smith, H. S. Udaykumar, and M. M. Rao. *Computational Fluid Dynamics with Moving Boundaries*. Taylor & Francis, Inc., Bristol, PA, USA, 1996.

(H. Kasumba) Johann Radon Institute for Computational and Applied Mathematics, Austrian Academy of Sciences, Altenbergerstrasse 69, A-4040 Linz, Austria

E-mail address: henry.kasumba@oeaw.at